

Optimization of integrated accurate ride-tide planning and vessel scheduling in multi-functional ports with long channels

Xinyu Zhang^a Wenqiang Guo^{a*} Zaili Yang^b Jingyun Wang^c Chengbo Wang^d

^a *Navigation College, Dalian Maritime University, Dalian, 116026, China*

^b *Liverpool Logistics, Offshore and Marine (LOOM) Research Institute, Liverpool John Moores University, Liverpool, UK*

^c *College of Transportation Engineering, Dalian Maritime University, Dalian, 116026, China*

^d *Department of Automation, University of Science and Technology of China, Hefei, 230031, China*

*Corresponding author: Wenqiang Guo

E-mail addresses: zhangxy@dlnu.edu.cn (Xinyu Zhang), guowenqiang@dlnu.edu.cn (Wenqiang Guo), Z.Yang@ljmu.ac.uk (Zaili Yang), wangjingyun@dlnu.edu.cn (Jingyun Wang), wangcb23@ustc.edu.cn (Chengbo Wang)

Abstract: Driven by economic globalization and the reduction of transport costs, “large-scale vessels” and “multi-functional ports” have emerged as the new paradigm in marine transportation. Within this context, traditional ride-tide planning and common rule-based vessel scheduling methods sometimes become ineffective in optimizing navigational potential, leading to serious waiting problems for large-scale vessels and increasing port congestion. This paper aims to develop a new point-by-point ship ride-tide (PSRT) approach to address accurate ride-tide planning and vessel scheduling issues for a long channel in a multi-functional port. The method is developed based on coupling the vessel’s speed change and tidal level variation to determine accurate ride-tide planning for large-scale vessels. A mixed integer linear programming (MILP) model is presented, in which the vessel’s accurate tide ride, dynamic sailing speeds, and vessel scheduling priority are explicitly considered. Due to the computational inefficiency of the MILP model in large-scale scenarios, we decompose it into a master problem and several subproblems and develop an improved branch-and-price (B&P) algorithm with three enhanced methods to solve this model. Computational experiments for Huanghua Port show that the PSRT method extends available tidal time windows (ATTWs) for large-scale vessels by an average of 20% compared to the traditional single-point tide-ride approach for the same under keel clearance. Moreover, the proposed improved B&P algorithm significantly outperforms existing methods such as column generation, branch and bound, and an improved genetic algorithm as well as the port scheduling schemes adopted in reality. This study has effectively unlocked the navigational potential of long channels, making new contributions to enabling ports to accommodate and serve a greater number of large and ultra-large vessels.

Keywords: Multi-functional port; accurate ride-tide planning; vessel scheduling; long channel; improved brand-and-price.

1. Introduction

With the advancement of globalization and continuous expansion of international trade, large and ultra-large vessels have become pivotal in ocean freight transportation, aiming to boost transport capacity and reduce transportation costs. As of the end of 2022, Cape-size vessels represented 39.5% of the total transport capacity of dry bulk ships worldwide, and Very Large Crude Carriers (VLCCs) constituted 40.4% of the global tanker fleet. The proportion of new orders for container ships with a capacity of over 17,000 TEU rose from 12.2% in 2021 to 22.7% in 2023 (Clarksons, 2023). To accommodate these large vessels, ports are extending their channels further offshore. Considering the nature of tides, tidal range variations, and actual navigational conditions, this article categorizes channels longer than 10 nautical miles as “long channels”. Many of the world’s ports now feature long channels, as illustrated in Table 1. In China, channels exceeding 10 nautical miles in length constitute 42% of the total. Specifically, ports like Zhanjiang, Huanghua, and Ningbo-Zhoushan have channel lengths exceeding 30 nautical miles.

Table 1

Length, tides, and passing tonnage of long channels in some of the world's ports.

Name of the port channel	Length of channel (nm)	Ride-tide scheme	Maximum tidal range (m)	The tonnage of vessels sailing on tides (DWT/TEU)
The main channel of Zhanjiang Port	40.4	Single point	2.41	300,000 DWT
Huanghua Comprehensive Port channel	34.0	Single point	3.26	200,000 DWT
Ningbo Zhoushan Port channel	30.0	Single point	4.70	150,000 DWT
The main channel of Lianyungang Port	28.5	Single point	6.90	250,000 DWT
Guangzhou Port Nansha channel	27.0	Single point	4.11	120,000 DWT
Shanghai Yangshan Port channel	26.4	Single point	4.40	200,000 DWT
Qingdao Port Qianwan channel	25.5	Single point	6.06	100,000 DWT
Tianjin Port channel	23.8	Single point	6.12	250,000 DWT
The main channel of Xiamen Port	18.8	Single point	6.92	150,000 DWT
Panjin Port Rongxing channel	15.6	Single point	6.14	100,000 DWT
Shenzhen Western Port channel	12.8	Single point	3.44	100,000 DWT
Manila Port channel	27.0	Single point	2.50	10,000 TEU
Rotterdam Port channel	26.6	Single point	5.00	150,000 DWT
Antwerp Port channel	18.8	Single point	4.50	14,000 TEU
Singapore Port channel	11.3	Single point	2.20	350,000 DWT
Wellington Port channel	10.0	Single point	1.90	150,000 DWT

The navigational effectiveness of vessels, significantly influenced by the unique geographic characteristics of the long channel and the complex interrelated traffic activities at the multi-functional port, can be attributed to three key factors:

(1) The current methods used to determine ride-tide planning for large-scale vessels are often questionable. Typically, large-scale vessels navigate into and out of a port during specified time windows to ensure sufficient water depth. The prevalent practice is to use a single-point tide gauge station to estimate the associated tide level throughout the entire channel and then define the known and constant available tidal time windows (ATTWs) for vessels, known as "single-point ride-tide". However, since these tide gauges are located in coastal areas, they could not always accurately capture significant variations in tidal levels along a long channel. For example, as depicted in Fig. 1, at midnight on June 1, 2020, the tidal level at a real illustrative channel entrance was measured as 192 cm, whereas it was 240 cm at the inner end of the channel, indicating a variance of 48 cm (i.e. 25% in terms of the ratio).

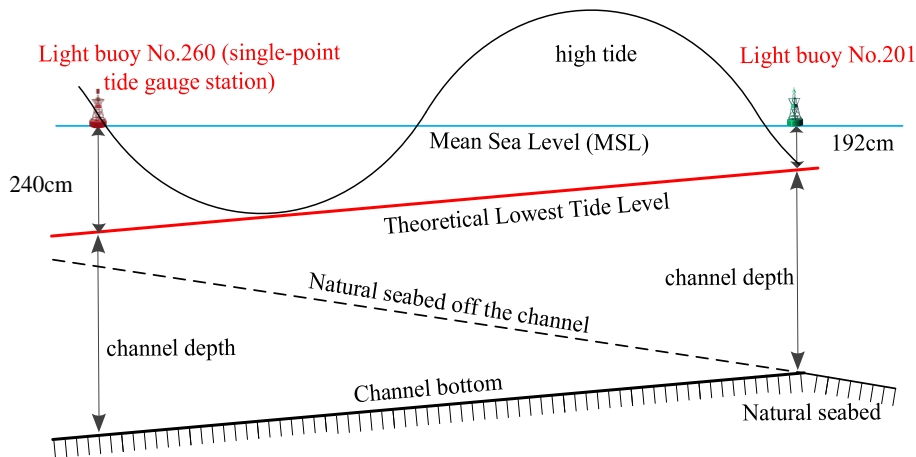


Fig. 1. Differences in tidal levels in a long channel.

(2) Complex patterns of vessel sailing speeds present challenges for vessel scheduling. When developing a vessel scheduling plan, an average speed is typically used to estimate vessel sailing time within a channel. However, as the channel length exceeds 10 nm, the vessel's sailing duration in the channel becomes significant, and the speed changes become more influential and complicated. In this case, the average speed couldn't effectively represent the

1 actual speed of the vessel. Therefore, it is inaccurate to use the average speed to estimate the sailing duration of
2 vessels in the channel, resulting in a significant impact on vessel scheduling. Furthermore, due to the prolonged
3 acceleration and deceleration processes required for large-scale vessels, relying solely on average speed to estimate
4 duration is an ineffective option. For example, a bulk carrier (MMSI: 414278000) entered Huanghua Port via the
5 channel on April 22, 2021. The length of the Huanghua Port channel is approximately 32 nautical miles. According
6 to 1863 AIS data points, the vessel's average sailing speed was 8.16 kn, which leads to an estimated sailing time of
7 $32 \div 8.16 = 3.92$ h. However, the actual sailing duration in the channel was 4.53 h (from 14:57 to 19:29). The differ-
8 ence between the two is approximately $(4.53 - 3.92) \div 3.92 = 15.56\%$. This demonstrates that using average speed to
9 estimate the sailing time in the channel results in a significant error.

10 (3) Vessel priority imposes constraints on vessel scheduling. Multi-functional ports often include terminals han-
11 dling bulk cargo, containers, dangerous goods, and so on. Various types of vessels utilize the same channel for entries
12 and departures. Given the distinct cargo attributes and safety protocols, dangerous goods vessels are given higher
13 priority in scheduling. These vessels require larger safety zones to minimize risks during navigation and berthing,
14 and these vessels need precise management of their transit speed and time to ensure they can berth and operate on
15 time. What's more, delays in entering or exiting ports can lead to significant repercussions, affecting not only daily
16 life but also industrial activities. For example, delays in berthing and unloading LNG vessels may result in energy
17 shortages in downstream cities and disrupt industrial production.

18 To enhance vessel navigation efficiency in long channels, port authorities have been undertaking a series of
19 successive channel dredging projects. However, such dredging requires significant time and financial investments
20 (Corry and Bierwirth, 2019). Additionally, many channels face geographical and environmental constraints that ren-
21 der channel dredging impractical in the short term. Therefore, improving the operations and management of long
22 channels in a multi-functional port becomes a crucial and beneficial approach to optimizing navigational potential
23 and reducing vessel waiting time.

24 In light of the foregoing, this paper focuses on accurate ride-tide planning and vessel scheduling for a long
25 channel in a multi-functional port. The contributions of this study are as follows:

26 (1) This study provides a point-by-point ship ride-tide (PSRT) approach to address the weaknesses exposed by
27 the traditional single-point ride-tide approach in long channels. Our findings demonstrate that the new method can
28 extend ATTWs by an average of 20% for large-scale vessels compared to conventional methods. It addresses the
29 issue of inaccurate ATTWs calculations due to substantial tidal level variations and vessel speed variations along long
30 channels. This allows the port to accommodate and service larger tonnage vessels without the need for deeper channel
31 dredging.

32 (2) This paper study involves the accurate ride-tide planning and vessel scheduling problem for a multi-func-
33 tional port with a long channel. Some important factors, such as tidal factors, speed change, and scheduling priority,
34 are widely considered in particular. However, they have never been comprehensively and systematically studied in
35 the literature. This study fills the gap by modeling industrial practice. A mixed integer linear programming (MILP)
36 model is developed for the problem. This model is capable of modeling the vessel movements within the long channel.

37 (3) The model is reformulated as a set-partitioning formulation. An improved branch and price (B&P) algorithm
38 is then presented to solve the set-partitioning formulation. Several enhancement methods, including the initial solu-
39 tion generation strategy based on the scheduled time-first variable neighborhood search (STFVNS) algorithm, sub-
40 problem solving method based on an improved label-setting algorithm, and a branched strategy for the original prob-
41 lem variables, are designed to improve the performance of the B&P algorithm.

42 The subsequent sections of this paper are organized as follows: [Section 2](#) provides a review of the literature.
43 [Section 3](#) introduces the PSRT method for vessels. [Section 4](#) describes the vessel scheduling model. [Section 5](#) details
44 the development of an improved B&P algorithm for this problem. Numerical and comparative experiments are con-
45 ducted in [Section 6](#), followed by the conclusion in [Section 7](#).

2. Literature review

In ride-tide planning and vessel scheduling, researchers have made significant efforts to enhance the efficiency of vessel inbound and outbound processes, such as developing quality models and efficient algorithms to obtain the optimal scheduling plan (Wang and Meng, 2017; Dulebenets et al., 2021; Ksciuk et al., 2023; Meng et al., 2024). Such as Yang et al. (2023) developed a model to minimize total vessel bunker costs and delay penalties by optimizing vessel schedules at waterway bottlenecks. La Scalia et al. (2023) proposed an optimization model that balances mandatory and optional maritime transport tasks to maximize profits and minimize carbon emissions, demonstrated through a case study involving the Aeolian Islands. Zhang et al. (2024) presented a MILP model to optimize vessel scheduling considering the variations in water discharge, using a multi-population genetic algorithm, demonstrated through a case study of the Three Gorges Dam to enhance transportation efficiency and navigational safety. Zhao et al. (2024) introduced a multi-objective optimization model to enhance vessel voyage scheduling for ore transportation by addressing uncertainties in voyage duration, aiming to maximize transfer volume and minimize operational costs using advanced algorithms and validation methods. Jiang et al. (2024) presented a multi-objective optimization model for the efficient scheduling of port resources, addressing the increasing demand and scheduling pressures in bulk cargo ports, with a focus on reducing carbon emissions. This section will highlight some of the most relevant and cutting-edge research.

2.1. Vessel ride-tide planning

Precisely calculating the ATTWs is essential and fundamental for realizing accurate ride-tide planning for vessels. Qiang et al. (2018) proposed a method for calculating ATTWs based on observed tidal data, offering data support for the navigation of large-scale vessels. Zhang et al., (2019) presented a model and algorithm for vessel ride-tide planning in a two-way channel, considering tidal depth variations affecting vessel drafts. The goal is to minimize total waiting time, with a case study on the Yangtze River estuary validating its efficiency compared to other scheduling methods (FCFS, RS, LDVF, and manual). Qiao et al. (2020) conducted a study on ATTWs calculation using different types of tidal data from tide-gauge stations near the coast of China. They concluded that ATTWs decreased from diurnal to semi-diurnal tide. Building on accurate tidal data, Zhang et al. (2022) proposed an adaptive duration arrangement calculation method aimed at improving ATTWs calculation accuracy. Zhong et al. (2022) developed a bi-objective MILP model for green tugboat ride-tide planning to minimize completion time and fuel consumption. The model accounted for ATTWs and used the Nondominated Sorting Genetic Algorithm II (NSGA-II) for a solution. Noshokaty (2023) addressed en-route bunkering, late port arrivals, and tide effects in liner operations. The study used a mixed continuous-integer linear programming model to optimize cargo mix, maximizing stochastic gross profit per day. Zhao et al. (2023) addressed the barge planning problem in tidal-affected narrow channels. They proposed a MILP model to minimize overall completion time and introduced a variable neighborhood search (VNS) algorithm to enhance computational efficiency. Liu et al. (2024) proposed a MILP for vessel ride-tide planning in restricted two-way channels to improve port efficiency. The model minimizes total delay costs by optimizing vessel entry and exit times, considering factors like tides, avoidance, and safety distances. Gao et al. (2024) proposed a MILP model for tramp vessel planning, considering tidal influences and nonlinear wait times. They used a B&P framework, decomposing the problem into a master problem and some subproblems with a speed-optimized labeling algorithm. These studies primarily rely on tidal data from single tide-gauge stations and tend to engage a strong assumption on a uniform tidal height distribution along a channel when calculating ATTWs. However, tidal levels could exhibit substantial variations along the channel's length, especially in those spanning tens of nautical miles, resulting in significant differences in tide heights at different locations simultaneously. Therefore, the state-of-the-art methods of ATTWs calculation fall short of meeting the accuracy and applicability demands for large vessels sailing in long channels.

2.2. Vessel scheduling

Scholars have conducted in-depth studies on the vessel ride-tide scheduling problem. Currently, most literature proposes scheduling models that utilize tidal water levels from single-point tide gauges to calculate ATTWs, treating them as known and constant time slots (Du et al., 2015; Dadashi et al., 2017; De et al., 2017; Zhen et al., 2017; Lalla-Ruiz, 2018; Jia et al., 2019). This approach significantly limits scheduling efficiency, especially in multi-functional ports accommodating different vessel types. The reason for this limitation is that, compared to a short channel, there is a significant difference in tidal heights at different locations within a long channel at the same time. In such cases, if the ATTWs are considered as constant time slots, large vessels must wait until their draft is less than the minimum water depth within the channel before being scheduled to enter or leave the port. This results in additional waiting time for large vessels.

The dynamic variation of sailing speed is also an important factor to consider when studying the vessel scheduling problem in multi-functional ports (Yan et al., 2020; Wu, 2020). Sailing speed is closely linked to the accuracy of calculating channel transit time and establishing safe temporal intervals between successive vessels. Moreover, dynamic variations in vessel speed affect the accuracy of predicting ride-tide times. Currently, most studies use the average speed to calculate channel transit times (Le Carrer et al., 2020; Özlem et al., 2021; Liu et al., 2021; Li et al., 2022). This method works well for single-functional ports or short channels where vessel speed changes little (Liu et al., 2021). However, the varying and dynamic sailing speeds of different vessel types and tonnages present challenges in multi-functional ports, particularly along long channels. Relying solely on average speed for calculating channel transit times and safety intervals is inadequate, impeding the development of an effective port scheduling plan and potentially leading to port congestion.

Vessel scheduling priority is another crucial aspect in addressing the vessel scheduling problem in multi-functional ports. The predominant research approach for vessel scheduling priority involves prioritizing vessels based on several factors, including the estimated time of arrival and departure (ETA and ETD), and specific vessel attributes such as tonnage, size, maneuverability, and berth proximity (Hsu et al., 2008; Zhang et al., 2017; Tang et al., 2022). Common rules include the first-come-first-serve and prioritizing larger-scale vessels for entry and exit. However, these methods are generally suited to single-functional ports and primarily focus on container ships and bulk carriers, with less attention given to the scheduling of dangerous goods vessels. Research on this topic often concentrates on a single category of dangerous goods vessels (Halvorsen-Weare et al., 2013; Halvorsen-Weare et al., 2013). Safety concerns lead to excessively large mobile safety zones around these vessels, often lacking optimal adaptability to actual navigational conditions. This approach neglects potential impacts on other vessels and the overall scheduling plan.

Table 2 compares the differences in the factors considered in this study and previous literature. Regarding tidal factors, previous studies have regarded ATTW as a known and constant time window, while this study designed a PSRT method to accurately calculate ATTW based on the tidal changes in the channel. Regarding vessel speed factors, previous studies mostly regarded the vessel speed as a uniform speed or used the average speed. In contrast, this study designed a speed mining algorithm for accumulated voyage distance, fitting the function curve of speed and distance, and more accurately reflecting the speed changes of the vessel in the channel. Regarding the scheduling priority of dangerous goods ships, most of the existing studies did not consider the specific need for dangerous goods ships to enter and leave the port on time, while this study took this specific need into account.

1 **Table 2**

2 A comparison table showing the differences in specific considerations between this paper and other literature.

Related research	Factors to consider		
	Tidal factor	Vessel speed factor	Priority factors for dispatching dangerous goods vessels
Corry & Bierwirth (2019)	Directly use a known and constant ATTW	Using the average speed	Not considered
Xiao et al., (2023)	Not considered	Assuming a uniform speed	Not considered
Du et al., (2015)	Directly use a known and constant ATTW	Assuming a uniform speed	Not considered
Dadashi et al., (2017)	Directly use a known and constant ATTW	Assuming a uniform speed	Not considered
Zhen et al., (2017)	Directly use a known and constant ATTW	Using the weighted average speed	Not considered
Lalla-Ruiz et al., (2018)	Directly use a known and constant ATTW	Using the average speed	Not considered
De et al., (2017)	Directly use a known and constant ATTW	Using the average speed	Not considered
Jia et al., (2019)	Directly use a known and constant ATTW	Assuming a uniform speed	Not considered
Le Carrer et al., (2020)	Directly use a known and constant ATTW	Using the weighted average speed	Not considered
Özlem et al., (2021)	Directly use a known and constant ATTW	Using the average speed	Not considered
Liu et al., (2021)	Directly use a known and constant ATTW	Assuming a uniform speed	Not considered
Li et al., (2022)	Directly use a known and constant ATTW	Assuming a uniform speed	Not considered
This study	Accurately calculate ATTW by PSRT method	Speed-distance function curve	Taking into account the specific needs of dangerous goods ships to enter the port on time

3 This paper thus addresses the accurate ride-tide planning and vessel scheduling problem for a long channel in a
4 multi-functional port, based on a more comprehensive and realistic consideration of vessel movements and operations.
5 This paper proposes a PSRT method, which, by analyzing the relationship between vessel navigation speed and distance
6 within long channels, reconstructs the coupling relationship between vessel speed and tidal levels through the
7 discretization of long channels into finely segmented routes. A MILP model is presented, capable of encapsulating
8 the characteristics of vessel traffic behavior in the long channels of multi-functional ports, thereby enhancing the
9 modeling of vessel movements within the port. An improved B&P algorithm is introduced to obtain near-optimal
10 solutions. To meet the time-sensitive requirements of port operations, several enhancement methods are proposed to
11 enhance the performance of the algorithm. The problem addressed in this paper is significantly more realistic and
12 innovative compared to previous studies. The proposed PSRT method not only accurately calculates but also effectively
13 extends the ATTWs, thus providing valuable guidance for port operations and the servicing of larger-scale
14 vessels. The proposed model can serve as a useful tool for port operators to formulate an optimal scheme for vessel
15 entry and exit from the port, considering a broader range of factors such as tidal influences, vessel types, and navigational
16 speeds.

17 3. The PSRT method

18 In this section, a PSRT method is designed to finely solve ATTWs for vessels by discretizing the long channel
19 into some segments and considering the influence of speed changes. The channel is divided into some segments, each
20 of which is one nautical mile long, primarily based on considerations of tidal height forecasting accuracy and vessel
21 navigation safety. This finer segmentation allows for a more precise calculation of tidal height data, thus better reflecting
22 the actual water level changes along the entire channel. However, given that large vessels typically measure
23 approximately 300 meters in length, it is necessary to maintain a safety distance equivalent to 6 times their length
24 during navigation within the channel, which corresponds to approximately one nautical mile. Therefore, segments
25 shorter than one nautical mile would impose an unnecessary computational burden for tidal height calculations, while
26 segments longer than one nautical mile may fail to accurately reflect the actual water level changes along the entire

1 channel, thereby affecting the accuracy of ATTWs calculations. Hence, dividing the channel into segments of one
 2 nautical mile ensures both the accuracy of tidal height calculations and the consideration of practical navigation safety
 3 factors.

4 3.1. Mining the dynamics of vessel speed variation

5 Understanding the dynamics of vessel speed variation in a long channel is essential for accurately calculating
 6 ATTWs. To this end, we have developed a sailing speed mining algorithm based on voyage accumulation. The algo-
 7 rithm's pseudocode is presented as [Algorithm 1](#).

Algorithm1: Sailing Speed Mining Algorithm Based on Voyage Accumulation

Input: "Initial vessels table" - Initial Automatic Identification System (AIS) data of vessels from the hiFleet (URL: <https://www.hifleet.com/>), covering the period from February 1, 2021, to March 1, 2023.

Output:

p : Function representing speed-voyage relationship for inbound vessels
 q : Function representing speed-voyage relationship for outbound vessels

1 Function: AIS data extraction, cleaning, identification, storing (Initial vessels table)

```

2 "Table1" ← Create an empty table
3 while the "Initial vessels table" is not empty do
4     if vessel speed < 0 or vessel speed > 30 kn then
5         Delete these AIS data:
6     end if
7     if Latitude > 90° or Longitude > 180° then
8         Delete these AIS data:
9     end if
10    if |(speedi - speedi-1)/(timei - timei-1)| < threshold then
11        Delete these AIS data:
12    end if
13    Save the remaining AIS data into "Table1"
14 end while
15 End Function

```

16 Function: Identify inbound and outbound vessels (Table 1)

```

17 Determine the true bearing of the channel as:  $\varphi_1$ 
18 Read the vessel's course from "Table 1" as:  $\varphi_2$ 
19 for each vessel in "Table 1" do
20     if  $\varphi_2 \in \varphi_1 \pm 10^\circ$  then
21         Save the AIS data into "Table 2" (for inbound vessels)
22     end if
23     if  $\varphi_2 \in \varphi_1 \pm 180^\circ$  then
24         Save the AIS data into "Table 3" (for outbound vessels)
25     end if
26 end for
27 End Function

```

28 Function: Fit speed-voyage relationship using cubic B-spline interpolation (Table 2 and Table 3)

```

29 Calculate the distance:
30  $Z = 1852.25 \times \sum_{i=1}^n \sqrt{(x_n - x_{n-1})^2 + (y_n - y_{n-1})^2}$ ,  $i = 1, 2, \dots, n$ ;  $Z$  represents the voyage, measured in nautical miles:
31 Fit the speed-voyage relationship for inbound vessels using cubic B-spline interpolation, denoted by  $p$ 
32 Fit the speed-voyage relationship for outbound vessels using cubic B-spline interpolation, denoted by  $q$ 
33 End Function
34 Return  $p$  and  $q$ 

```

1 The specific explanation for [Algorithm 1](#) is as follows:

2 **Step 1: Automatic Identification System (AIS) Data Management** - Extract, clean, identify, and store AIS
3 data. Remove data points with vessel speeds less than zero or abnormally high values (typically exceeding 30 knots,
4 especially near ports). Eliminate data points with a longitude greater than 180 degrees or a latitude greater than 90
5 degrees. Filter out densely sampled data points. Due to non-uniform time sampling intervals, AIS data points may
6 exhibit discontinuities. During phases of high or moderate vessel speeds where velocity changes are minimal, densely
7 sampled points can distort statistical analysis. Thus, data points representing minimal changes in vessel speed will be
8 removed. This involves calculating the rate of change of vessel speed between consecutive points by dividing the
9 speed difference by the time interval between them. If the rate of change is below a predefined threshold, the preced-
10 ing data point will be deleted. The threshold is set to a natural number with a value of three ([Zhang et al., 2019](#)). Then,
11 store the filtered data in a newly created table, “Table1”.

12 **Step 2: Vessel Direction Identification** - Identify inbound and outbound vessels. Firstly, determine the true
13 bearing of the channel, denoted as φ_1 . Then, retrieve the vessel’s heading from “Table 1”, denoted as φ_2 . If $\varphi_2 \in$
14 $\varphi_1 \pm 10^\circ$, the vessel is considered to be in an inbound state; if $\varphi_2 \in (\varphi_1 \pm 180^\circ)$, it is considered outbound ([Chen](#)
15 [2023](#)). Additionally, store the dynamic data points of inbound and outbound vessels in “Table2” and “Table3”, re-
16 spectively.

17 **Step 3: Speed-Voyage Relationship Modeling** - Fit the speed-voyage relationship using cubic B-spline inter-
18 polation ([Shafiq et al., 2022](#)). Utilize the longitude and latitude coordinate (x_1, y_1) of the vessel’s anchor point
19 (berth) as the starting point for inbound (outbound) vessels, and the current longitude and latitude coordinates
20 $(x_i, y_i), i = 1, 2, \dots, n$ of the vessel as the endpoint. Adopt the formula $Z = 1852.25 \times$
21 $\sum_{i=1}^n \sqrt{(x_n - x_{n-1})^2 + (y_n - y_{n-1})^2}, i = 1, 2, \dots, n$ to calculate the cumulative voyage traveled by the vessel during
22 its inbound or outbound navigation. Employ the cubic B-spline algorithm to fit the functional relationships of vessel
23 speed and voyage traveled during inbound and outbound navigation separately. These fitted relationships are denoted
24 as p and q , respectively.

25 3.2. Accurate calculation of ATTWs

26 This subsection accurately calculates ATTWs based on functions p and q . The method calculates the start and
27 end times of ATTWs based on the duration of vessel tide riding and the relationship between the actual water depth
28 of the segments and the vessel’s required water depth, i.e., draft plus under keel clearance (UKC). The pseudocode
29 for accurately calculating ATTWs is outlined in [Algorithm 2](#). The specific description is provided as follows:

30 **Step 1:** Obtain the time and voyage traveled by vessels during navigation within the channel. Firstly, calculate
31 the current vessel speed corresponding to its position using the function p . Then, continuously update the time and
32 voyage traveled at 1-minute intervals until the vessel completely exits the channel. Record the corresponding time
33 and voyage traveled in Tables T and S, respectively.

34 **Step 2:** Compute the time required for a vessel to travel through each segment. Discretize the long channel into
35 evenly spaced channel segments of one nautical mile each. For each segment i , locate the positions s_{i1} and s_{i2}
36 where the vessel enters and leaves the current segment, respectively, in Table S. Corresponding times t_{i1} and t_{i1}
37 are found in Table T. Finally, calculate the duration it takes for the vessel to traverse each segment, denoted as $t_{i1} -$
38 t_{i2} .

39 **Step 3:** Compute the start and end times of the ATTW. Firstly, retrieve the tidal height data for each minute from
40 “Table 4”, and the water depth for each segment is obtained from “Table 5”. Then, for each time point, determine
41 whether the sum of tidal height and every segment’s depth exceeds the vessel’s draft plus the UKC. If at time point
42 t , from the vessel’s entry into the channel until its exit completes, the condition holds true, then t is identified as the
43 start time of the ATTW. If at a time point t' after t , the condition is not met, then t' is identified as the end time of
44 the ATTW.

Algorithm 2: Accurate calculating ATTWs

Input: “Table 4”: Tidal data for every point every minute. l : The length of the channel. d : vessel’s draft. Under Keel Clearance: 15% of the vessel’s draft. “Table 5”: The water depth for each segment of the channel. tp : Time steps.

Output: $[t, t']$: available tidal time window.

```
1 Function: Obtain the corresponding time and distance
2   Initialize empty lists T and S to store time and distance
3   Compute the initial velocity  $v$  for the current position of the vessel
4   While the last distance in S is less than the channel length  $l$ 
5     Append  $(t[-1] + tp)$  to T
6     Append  $(s[-1] + v[-1] * tp)$  to S
7   End While
8   Return T, S
9 End Function

10 Function: Compute the time required for a vessel to travel through each segment
11   Compute “range” as the rounded-up value of the channel length  $l$ 
12   Initialize an empty list “tres” to store the time required for each segment
13   For each segment  $i$  from 1 to “range”
14     Find all distances in S less than  $i$  and store them in  $ts$ 
15     Compute the length of  $ts$ , named  $tt$ 
16     Append  $tt$  to “tres”
17   End For
18   Return tres
19 End Function

20 Function: Calculate the start and end times of the available tidal time windows (ATTWs)
21   Read tide_high and time from “Table4” and water_depth from “Table5”
22   Get the length of the course_depth list, named “coursenum”
23   Get the length of the time list, named “trange”
24   Initialize empty lists use_start_time and use_end_time to store start and end times
25   For each time point  $i$  from 1 to “range”
26     For each course_depth  $j$  from 1 to “coursenum”
27       If  $(\text{tide\_high} + \text{course\_depth}) > \text{water\_depth} + \text{UKC}$ 
28         Append the start time to use_start_time
29       Else
30         Append  $(\text{start} + 1)$  to use_end_time
31       End If
32     End For
33   End For
34   Determine the first element of use_start_time as  $t$ 
35   Determine the first element of use_end_time as  $t'$ 
36   Return  $[t, t']$ 
37 End Function
```

1 **4. The vessel scheduling model**

2 Upon the vessel’s arrival at the port, it will anchor at the designated anchorage area until receiving authorization
3 from the Vessel Traffic Service (VTS) center to weigh its anchor. Subsequently, the vessel will sail through the chan-
4 nel to its assigned berth for loading or unloading operations. When the vessel submits a departure request, the port
5 will forward the vessel’s name, berth location, and other pertinent information to the VTS center for review. The
6 vessel may only sail through the channel to exit the port upon receiving clearance. It is evident that timely entry and
7 departure significantly affect the operational efficiency of both the vessel and the port. Extended wait in the anchorage
8 increases anchoring costs, while delays beyond the estimated departure time escalate berthing costs. In this paper, the
9 combined additional anchoring costs and increased berthing costs are termed waiting costs. It should be emphasized
10 here that berthing costs include the penalty for the vessel to leave later than the latest time.

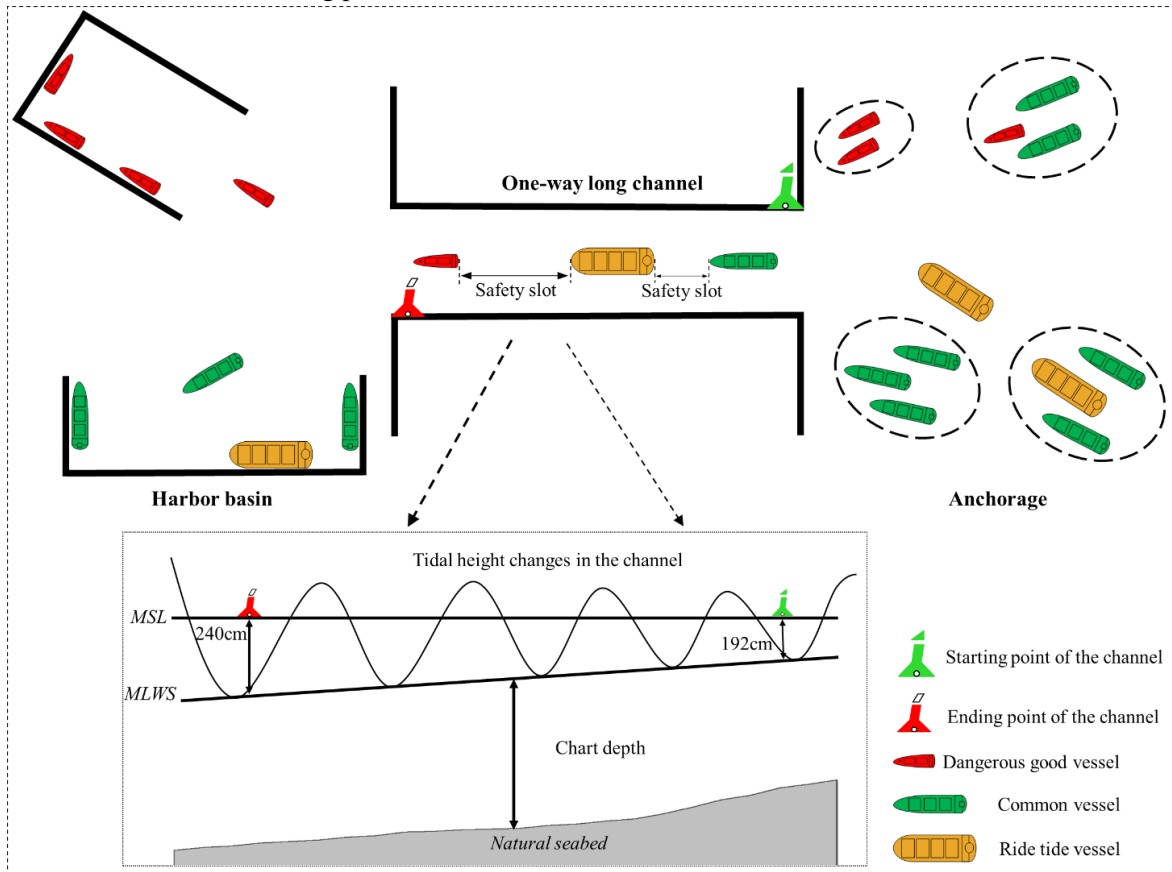
1 Therefore, the problem involves optimizing vessel scheduling in a multi-functional port with a long channel. As
 2 shown in Fig. 2, given the information regarding the vessel's estimated time of arrival, the accurate tidal planning,
 3 the change in vessel speed, the scheduling priority of dangerous goods vessel, and the maintenance of a safe slot
 4 between two vessels are taken into consideration, and the waiting costs of vessels are minimized by determining the
 5 optimal scheduling scheme. In this study, the scheduling scheme is defined as: the time arrangement for vessels to
 6 enter or leave the seaport, aiming to minimize vessels' total waiting costs while adhering to operational constraints.
 7 In this study, the channel type is a one-way channel, meaning vessels traveling in opposite directions cannot pass at
 8 the same time. The entire planning period is divided into multiple entry and exit periods, which alternate. Vessels can
 9 only complete the entry process during the entry periods and the exit process during the exit periods.

10 To make this research problem clear and relevant, but not complicated by unessential features, we establish the
 11 following research boundaries and assumptions:

12 (1) Assumes no external factors (e.g., unexpected weather changes, technical failures, or emergencies) would
 13 impact the vessels' navigation or scheduling. The port is also assumed to be operating at full capacity with no delays
 14 due to factors like port congestion or berth unavailability beyond the scope of the model.

15 (2) Assumes that safety slots between vessels are fixed and based on a simplified minimum distance for safety.
 16 These safety slots do not account for varying environmental conditions, such as reduced visibility or unpredictable
 17 currents, which might affect the required distance between vessels.

18 (3) Assumes that qualified pilots and tugboats can operate on time and that other human and environmental
 19 factors do not affect the scheduling process.



20 **Fig. 2.** An illustrative example of the vessel scheduling for a multi-functional port with a long channel.
 21

22 **4.1. Notation**

Sets and indexes

I Set of vessels, $I = I^D \cup I^O$, $i \in \{1, 2, \dots, |I|\}$;

I^D Set of dangerous goods vessels, $i^D \in \{1, 2, \dots, I^D\}$;

- I^O Set of other vessels, $i^O \in \{1,2, \dots, I^O\}$;
- E Set of arrival and departure time period, $e \in \{1,2, \dots, |E|\}$;
- T Set of moments, $t \in \{1,2, \dots, |T|\}$;
- R Set of available tidal time windows (ATTWs), $r \in \{1,2, \dots, |R|\}$.

Parameters

- L The voyage distance from anchorage to berth, measured in nautical miles;
- l The length of the channel, measured in nautical miles;
- v_i The function describing the speed and voyage of vessel i from the anchorage to the berth;
- v'_i The function describing the speed and voyage traveled by the vessel i within the long channel;
- k The safety slot between adjacent vessels, measured in minutes;
- O_i The duration of vessel i berthing operations, measured in minutes;
- ρ The time interval between adjacent ATTWs, measured in minutes;
- TO The length of arrival and departure period.
- ARR_i The moment when vessel i arrives at anchorage;
- ETD_i The estimated time of departure of vessel i ;
- $[ear_i^r, lat_i^r]$ The start and end moments of the ATTW r for the vessel i ;
- c_i The unit berthing cost for vessel i at the berth, including the penalty for the vessel to leave later than the latest time;
- ω_i The unit anchoring cost for vessel i at the anchorage;
- $RT_i = 1$ Vessel i requires ride tide for entering and leaving port and equals to zero otherwise;
- $\partial_e = 1$ e is the arrival period and equals to zero otherwise;
- $ws_{ie} = 1$ Vessel i enters the port in period e and equals to zero otherwise;
- $wd_{ie} = 1$ Vessel i leaving the port in period e and equals to zero otherwise;
- M A sufficiently large positive number.

Decision variables

- φ_{it} Set to one if t is within a time frame during which vessel i maintains a safe slot upon its entering port, i.e., $A_i - k < t < A_i + k, i \in I$ and to zero otherwise;
- ψ_{it} Set to one if t is within a time frame during which vessel i maintains a safe slot upon its leaving port, i.e., $D_i - k < t < D_i + k, i \in I$ and to zero otherwise;
- in_i^r Set to one if vessel i entering port in the r and to zero otherwise;
- out_i^r Set to one if vessel i leaving port in the r and to zero otherwise;
- A_i The moment vessel i begins entering port, i.e., the moment when the vessel weighs anchor;
- D_i The moment vessel i begins leaving port, i.e., the moment when the vessel departs from the berth;
- λ Set to one if the vessel i^O is scheduled after the vessel i^D and to zero otherwise;
- f_{it} Set to one if vessel i begins entering port at the moment t and to zero otherwise;
- g_{it} Set to one if vessel i begins leaving port at the moment t and to zero otherwise;
- α_i The duration of vessel i waits in the berth before leaving the port;
- β_i The duration of vessel i waits in the anchorage before entering the port.

1 4.2. Mathematical Model

2 Given the input parameters and decision variables, the MILP model can be formulated in the following manner:

$$\text{minimize } \sum_{i \in I} \alpha_i c_i + \beta_i \omega_i \quad (1)$$

Subject to

$$\sum_{i \in I} \varphi_{it} \leq 1, \forall t \in T \quad (2)$$

$$\sum_{i \in I} \psi_{it} \leq 1, \forall t \in T \quad (3)$$

$$\varphi_{it_1} + M(1 - f_{it_2}) \geq 1, \forall i \in I, t_1, t_2 \in T, t_2 - k < t_1 < t_2 + k \quad (4)$$

$$\psi_{it_1} + M(1 - g_{it_2}) \geq 1, \forall i \in I, t_1, t_2 \in T, t_2 - k < t_1 < t_2 + k \quad (5)$$

$$A_i \geq ARR_i, \forall i \in I \quad (6)$$

$$D_i \geq A_i + O_i + L/v_i, \forall i \in I \quad (7)$$

$$\alpha_i = D_i - ETD_i, \forall i \in I \quad (8)$$

$$\beta_i = A_i - ARR_i, \forall i \in I \quad (9)$$

$$\sum_{e \in E} ws_{ie} * \partial_e = 1, \forall i \in I \quad (10)$$

$$M(1 - ws_{ie}) + A_i \geq 1 + TO * (e - 1), \forall i \in I, \forall e \in E \quad (11)$$

$$M(ws_{ie} - 1) + A_i + L/v_i \leq TO * e, \forall i \in I, \forall e \in E \quad (12)$$

$$\sum_{e \in E} wd_{ie} * (1 - \partial_e) = 1, \forall i \in I \quad (13)$$

$$M(1 - wd_{ie}) + D_i \geq 1 + TO * (e - 1), \forall i \in I, \forall e \in E \quad (14)$$

$$M(wd_{ie} - 1) + D_i + l/v'_i \leq TO * e, \forall i \in I, \forall e \in E \quad (15)$$

$$\sum_{r \in R} in_i^r = RT_i, \forall i \in I \quad (16)$$

$$\sum_{r \in R} out_i^r = RT_i, \forall i \in I \quad (17)$$

$$M(in_i^r - 1) + A_i \geq ear_i^1 + \rho(r - 1), \forall i \in I, \forall r \in R \quad (18)$$

$$M(1 - in_i^r) + A_i + l/v'_i \leq lat_i^1 + \rho(r - 1), \forall i \in I, \forall r \in R \quad (19)$$

$$M(1 - out_i^r) + D_i \geq ear_i^1 + \rho(r - 1), \forall i \in I, \forall r \in R \quad (20)$$

$$M(out_i^r - 1) + D_i + l/v'_i \leq lat_i^1 + \rho(r - 1), \forall i \in I, \forall r \in R \quad (21)$$

$$M\lambda \geq A_{i^D} - A_{i^0}, \forall i^0 \in I^0, \forall i^D \in I^D \quad (22)$$

$$\alpha_i \geq 0, \beta_i \geq 0, \forall i \in I \quad (23)$$

$$\varphi_{it}, \psi_{it}, in_i^r, out_i^r, \lambda, f_{it}, g_{it} \in \{0, 1\}, \forall i \in I, \forall t \in T, \forall r \in R \quad (24)$$

1 where objective (1) minimizes the total waiting costs for vessels, including additional anchoring costs and increased
2 berthing costs. The penalty for a vessel failing to leave the port on time is included in the additional berthing costs.
3 Constraints (2)-(3) ensure that two adjacent vessels maintain a safe slot during their entry and exit from the port. The
4 safety slot is necessary to avoid collisions and maintain smooth traffic flow within the port. Constraints (4) and (5)
5 are defined by defining variables φ_{it} and ψ_{it} to indicate whether vessel i is in a safe interval state with its neigh-
6 bors at a specific moment. Specifically, variable φ_{it} represents whether vessel i meets the safe interval condition
7 when entering the port, while ψ_{it} represents whether vessel i meets the safe interval condition when leaving the
8 port. Constraints (6) represent the related constraints on the beginning moment of the vessel inbound, ensuring that
9 this moment is greater than its arrival time at the anchorage. Constraints (7) represent the related constraints on the
10 beginning moment of the vessel outbound, ensuring that this moment is greater than the completion of its operations.
11 Constraint (8) defines variable α_i , i.e., the duration of vessel i waits in the berth before leaving the port, which is

1 the difference between the moment of vessel i begins leaving port and the estimated time of departure of vessel i .
2 Constraint (9) defines variable β_i , i.e., the duration of vessel i waits in the anchorage before entering the port, which
3 is the difference between the moment of vessel i begins entering port and the moment when vessel i arrives at
4 anchorage. Constraint (10) indicates that each vessel must select an arrival period for the arrival process. Constraints
5 (11) - (12) specify that the start and completion times of the vessel arrival must fall within the period range. Constraint
6 (13) indicates that each vessel must select a departure period for the departure process. Constraints (14) - (15) specify
7 that the start and completion times of the vessel departure must fall within the period range. Constraint (16) indicates
8 that ride tide vessels must choose a suitable ATTW to complete their entry into the port. Constraint (17) similarly
9 requires that ride tide vessels select a suitable ATTW to complete their departure from the port. Constraints (18) - (19)
10 ensure that the beginning and finishing moments of port entry for vessels riding the tide fall within the ATTW. Con-
11 straints (20) - (21) ensure that the starting and finishing moments of departure for vessels riding the tide also fall
12 within the ATTW. Constraint (22) ensures that vessels carrying dangerous goods are prioritized in the scheduling
13 process over other types of vessels. This prioritization is essential for ensuring safety and regulatory compliance in
14 port operations, as hazardous materials may require special handling and safety measures. Constraints (23) - (24)
15 define the domains of the decision variables, specifying the possible ranges for each decision variable. This ensures
16 that all variables are assigned valid values.

17 *4.3 Computational complexity analysis through reduction*

18 From the model, we can find that scheduling vessels in multi-functional ports requires simultaneous considera-
19 tion of ATTWs, vessel priorities, and navigational safety constraints. These factors introduce combinatorial complex-
20 ity as each vessel's entry and exit decisions depend on the schedule of other vessels. This subsection rigorously proves
21 the NP-hardness of the proposed problem by reducing it to the well-known Knapsack Problem. The Knapsack Prob-
22 lem, as shown in Kellerer et al. (2004), is a classical NP-complete problem. Additionally, the complexity of the full
23 model is analyzed to demonstrate the exponential growth of variables and constraints.

24 *4.3.1 Key complexity sources*

25 The problem involves optimizing vessel entry and exit schedules in a multi-functional port with the following
26 key complexities:

27 (1) Each large-scale vessel must enter or exit the channel within specific ATTWs to ensure adequate water depth.
28 Determining these ATTWs depends on dynamic tidal variations and vessel-specific constraints, making the feasibility
29 check computationally intensive.

30 (2) In a one-way long channel, vessels traveling in opposite directions cannot navigate simultaneously, adding
31 another layer of interdependency to the scheduling problem.

32 (3) The objective function includes minimizing waiting costs, which combine anchoring and berthing penalties.
33 These costs are linked to the start and completion times of each vessel's schedule, further complicating the decision-
34 making process.

35 *4.3.2 Reduction to the Knapsack Problem*

36 To rigorously prove the NP-hardness, the problem is reduced to the Knapsack Problem, a known NP-complete
37 problem. To simplify the reduction process, the following assumptions are made:

- 38 • All vessels have identical priorities;
- 39 • One-way channel constraints are ignored;
- 40 • Tidal variations are uniform and fixed.

41 These simplifications preserve the fundamental computational hardness of the problem, as they retain the core
42 structure and constraints relevant to NP-hardness analysis. Under these assumptions, the problem reduces to deter-
43 mining whether a feasible assignment of entry and exit times exists that satisfies the ATTW constraints for large
44 vessels while allowing other vessels to operate without such restrictions. Mapping to the Knapsack Problem:

- 45 • Items: Each vessel is treated as an item in the knapsack;
- 46 • Weights: A vessel's transit time corresponds to the weight of the item;

- Values: The inverse of a vessel's waiting cost corresponds to the item's value;
- Knapsack capacity: The total available scheduling time is the knapsack capacity.

The proof steps are as follows:

Step 1: Instance construction: We construct an instance of the proposed scheduling problem based on a given Knapsack Problem instance as follows:

(1) Items \rightarrow Vessels: Each item in the Knapsack Problem corresponds to a vessel. For example, Item 1 becomes vessel A , Item 2 becomes vessel B , and Item 3 becomes vessel C .

(2) Weights \rightarrow Transit Times: The weight w_i of each item corresponds to the transit time t_i of the corresponding vessel. For example, $t_A = 2, t_B = 3, t_C = 5$.

(3) Values \rightarrow Inverse Waiting Costs: The value v_i of each item corresponds to the inverse of the waiting cost c_i of the corresponding vessel. For example, $c_A = \frac{1}{6}, c_B = \frac{1}{10}, c_C = \frac{1}{15}$.

(4) Knapsack capacity \rightarrow Scheduling window: Such as, the knapsack capacity $C = 8$ maps to the total scheduling time window $T = 8$.

(5) Resulting scheduling problem: The objective is to minimize total waiting cost, i.e., Minimize $\sum_{i \in \{A,B,C\}} c_i x_i$, where $x_i = 1$ indicates vessel i is scheduled, and $x_i = 0$ otherwise. The constraints including:

- $\sum_{i \in \{A,B,C\}} T_i x_i \leq T$ (total transit time does not exceed the scheduling window);
- $x_i \in \{0,1\}$.

Step 2: Feasibility equivalence: A feasible solution to the Knapsack Problem corresponds directly to a feasible vessel scheduling plan:

(1) In the Knapsack Problem, selecting items 1 and 2 ($x_1 = 1, x_2 = 1, x_3 = 0$) results in a total weight of $w_1 + w_2 = 2 + 3 = 5$, which satisfies the capacity constraint ($5 \leq 8$).

(2) In the scheduling problem, scheduling vessels A and B ($x_A = 1, x_B = 1, x_C = 0$) results in a total transit time of $t_A + t_B = 2 + 3 = 5$, which satisfies the scheduling window constraint ($5 \leq 8$).

Thus, the feasibility of solutions in the Knapsack Problem directly translates to feasibility in the scheduling problem.

Step 3: Optimality preservation: The optimal solution to the Knapsack Problem provides the optimal scheduling plan:

(1) In the Knapsack Problem, selecting items 1 and 2 ($x_1 = 1, x_2 = 1, x_3 = 0$) maximizes the total value: $v_1 + v_2 = 6 + 10 = 16$.

(2) In the scheduling problem, scheduling vessels A and B ($x_A = 1, x_B = 1, x_C = 0$) minimizes the total waiting cost: $c_A + c_B = 6 + 10 = 16$.

The inverse relationship between item values and waiting costs ensures that maximizing the total value in the Knapsack Problem is equivalent to minimizing the total waiting cost in the scheduling problem.

Step 4: Conclusion: Since the Knapsack Problem is NP-complete, and the scheduling problem retains its computational hardness under this reduction, the full scheduling problem is at least as hard as the Knapsack Problem. Therefore, the scheduling problem is NP-hard.

In addition, in the model, the numbers of binary variables and big-M constraints are $O(N \times E + N^2)$ and $O(N^2 \times E + N \times E)$, respectively. The total number of binary variables in the model comes from two main components: vessel arrival and departure time selection, and the priority relationships between vessels. For the arrival and departure times, binary variables are introduced to indicate whether a vessel enters or leaves the port at a specific time step. The number of these variables is proportional to both the number of vessels N and the number of time steps E , giving a total of $O(N \times E)$ variables. For the priority relationships, binary variables are used to represent whether one vessel is scheduled before another, resulting in $O(N^2)$ variables due to the need to consider all vessel pairs. Combining both components, the total number of binary variables is $O(N \times E + N^2)$. The total number of big-M constraints in the model comes from three key components: safety distance, ATTW, and one-way channel constraints. The safety distance constraints ensure that each pair of vessels maintains a required distance at every time step,

1 resulting in $O(N^2 \times E)$ constraints. The tidal time window constraints, which regulate the vessels' entry and exit
2 times based on tidal conditions, contribute $O(N \times E)$ constraints. The one-way channel constraints, which prevent
3 vessels from traveling in opposite directions in the same channel, also require $O(N^2 \times E)$ constraints. Combining
4 these, the total number of big- M constraints is $O(N^2 \times E + N \times E)$. These factors result in an exponential expansion
5 of the feasible solution space, underscoring the NP-hard nature of the problem. Consequently, the rapid growth in
6 variables and constraints with problem size renders general-purpose solvers inadequate for large-scale instances.

7 **5. Solution approach**

8 Due to the substantial number of binary variables and big- M constraints in the model, directly solving it using
9 CPLEX is time-consuming and may not yield an optimal solution (i.e., an optimal scheduling scheme) within the
10 required time frame to meet operational demands. To address this, we present a set-partitioning formulation based on
11 a reformulation of the model, which is solved using the B&P algorithm embedded with three enhancement methods.
12 An examination of the model reveals that constraints (2)-(3) are coupled, while the remaining constraints exhibit a
13 diagonal chunking structure, allowing for independent solutions for each vessel. As a result, the model is decomposed
14 into a master problem (MP) and several subproblems (one for each vessel). The optimal solution derived from this
15 decomposition corresponds to the optimal scheduling scheme of the original problem. Therefore, the scheduling
16 schemes are generated by iteratively solving the MP and subproblems through the improved B&P algorithm.

17 *5.1. Set-partitioning reformulation*

18 In order to describe the MP accurately and clearly, the following notation is defined:

19 *Input Parameters:*

S_i Set of scheduling schemes for vessel i ;

a_i Scheduling scheme for vessel i , $a_i \in S_i$;

$\bar{\varphi}_{a_i}^t$ Set to one if in scheme a_i , t is within a time frame during which vessel i maintains a safe slot upon
entering port and to zero otherwise;

$\bar{\psi}_{a_i}^t$ Set to one if in scheme a_i , t is within a time frame during which vessel i maintains a safe slot upon
leaving port and to zero otherwise;

γ_{a_i} In scheme a_i , the duration of vessel i waits at the berth before leaving the port;

η_{a_i} In scheme a_i , the duration of vessel i waits at the anchorage before entering the port.

20 *Decision variables:*

K_{a_i} Set to one if the scheme a_i is chosen, and to zero otherwise.

21 The above parameters and variables are incorporated into the original model, resulting in the MP model through
22 transformation and collation as follows:

$$\text{minimize } \sum_{i \in I} \sum_{a_i \in R_i} (\gamma_{a_i} c_i + \eta_{a_i} \omega_i) K_{a_i} \quad (25)$$

$$\sum_{i \in I} \sum_{a_i \in R_i} \bar{\varphi}_{a_i}^t K_{a_i} \leq 1, \quad \forall t \in T \quad (26)$$

$$\sum_{i \in I} \sum_{a_i \in R_i} \bar{\psi}_{a_i}^t K_{a_i} \leq 1, \quad \forall t \in T \quad (27)$$

$$\sum_{a_i \in R_i} K_{a_i} = 1, \quad \forall i \in I \quad (28)$$

$$K_{a_i} \in \{0,1\}, \quad \forall i \in I \quad (29)$$

23 where the objective of function (25) is to minimize the total waiting costs of vessels. Constraints (26)-(27) guarantee

1 that two vessels in all schemes maintain a safe distance while navigating the channel. Constraint (28) stipulates that
 2 each vessel must select one specific scheme. The definitions of the variables involved are detailed in Constraint (29).
 3 Owing to the vast number of vessel scheduling schemes, solving the master problem becomes increasingly challeng-
 4 ing. Therefore, in line with the column generation algorithm, it is crucial to relax Constraint (29). This relaxation
 5 allows us to identify feasible schemes a_i that can be incorporated into the MP, leading to the formation of the re-
 6 stricted master problem (RMP).

7 Taking $\varpi, \theta, \vartheta$ as the dual variables of constraints (26)-(28), respectively, the RMP reduced cost is shown in
 8 Eq. (30).

$$(\alpha_i c_i + \beta_i \omega_i) - \sum_{t \in T} \varpi_t \varphi_{it} - \sum_{t \in T} \theta_t \psi_{it} - \vartheta_i \quad (30)$$

9 In each iteration of the column generation process, the subproblem focuses on identifying columns with negative
 10 reduced costs in the RMP and integrating them into the MP. Consequently, the objective function of the subproblem
 11 is defined by Eq. (31).

$$\text{minimize}(\alpha_i c_i + \beta_i \omega_i) - \sum_{t \in T} \varpi_t \varphi_{it} - \sum_{t \in T} \theta_t \psi_{it} - \vartheta_i \quad (31)$$

12 The constraints of each subproblem are listed as (4)-(22). In each subproblem, the subscript i remains unchanged,
 13 representing the corresponding vessel, thus, the number of subproblems equals the number of vessels. Each subprob-
 14 lem corresponds to a vessel scheduling scheme, which must satisfy constraints related to arrival and departure times,
 15 as well as scheduling priorities. Only solutions with an objective function value less than zero are eligible for inclu-
 16 sion in the main model for iterative solving. If no solutions meeting these criteria are found, then the optimal solution
 17 to the relaxed problem of the main problem has been identified. Additionally, according to duality properties, the dual
 18 variables ϖ and θ should be less than zero. When ϑ is less than or equal to zero, the main problem's reduced
 19 cost is greater than or equal to zero. In this case, there are no columns with reduced costs less than zero, making it
 20 unnecessary to solve the subproblems.

21 5.2. Improved branch and price (B&P)

22 Since the column generation algorithm only provides the optimal solution to the relaxed problem of the original
 23 issue and cannot ensure this solution is an integer, it is combined with branch-and-bound. This approach, known as
 24 branch-and-price, is used to solve the problem.

25 5.2.1 Framework of the improved B&P algorithm

26 As shown in Fig. 3, the enhanced methods embedded in the algorithm include:

- 27 • The scheduled time-first variable neighborhood search (STFVNS) algorithm is designed (see Section 5.2.2)
 28 to obtain a better initial scheme;
- 29 • In each subproblem, multiple columns with negative reduced costs are generated by an improved label-
 30 setting algorithm (ILSA) (see Section 5.2.3) and added to the RMP;
- 31 • A branched strategy is proposed (see Section 5.2.4) for the original problem variables to prevent the crea-
 32 tion of unbalanced enumeration trees and the introduction of new dual variables.

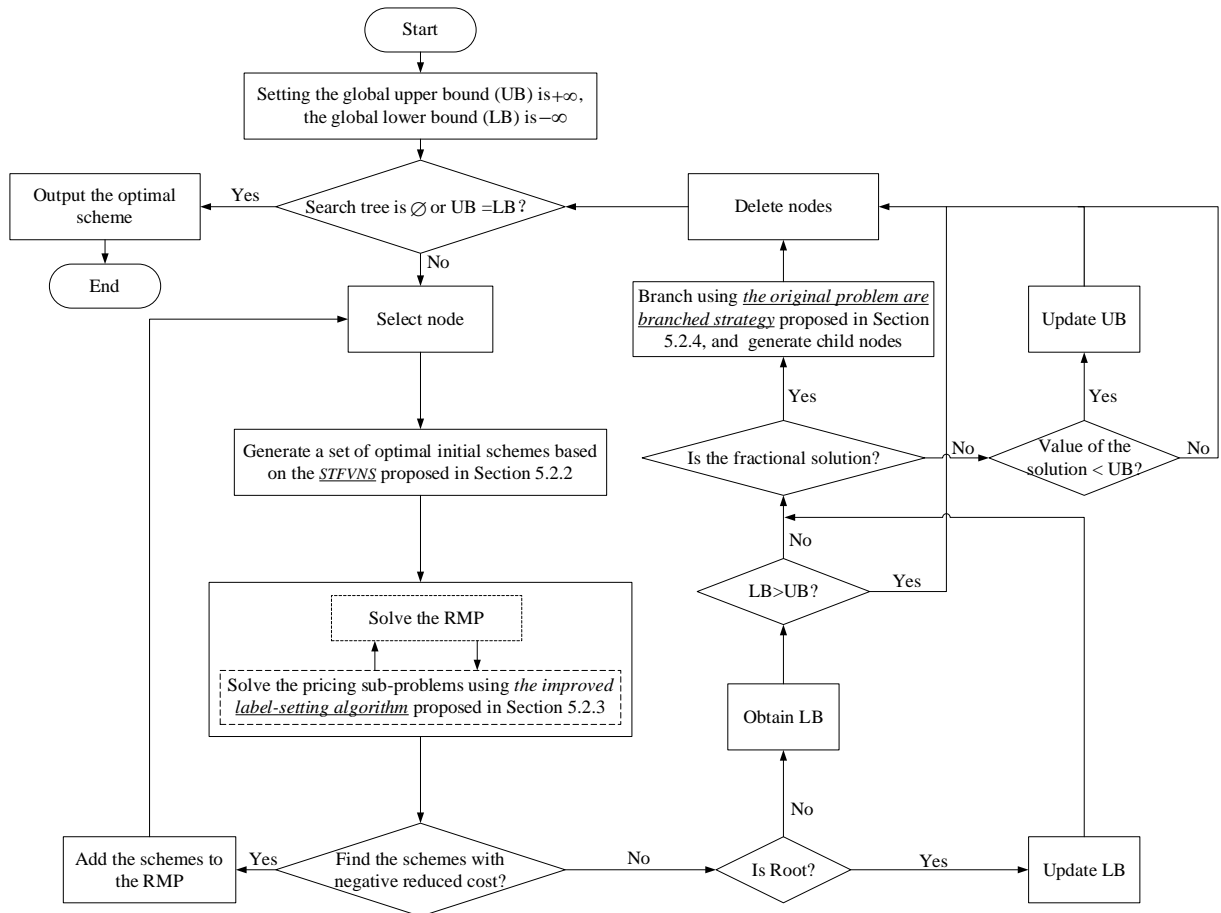


Fig. 3. Framework of the proposed improved B&P algorithm.

5.2.2. Initial scheme generation strategy based on STFVNS

The efficiency and convergence speed of the B&P algorithm highly depend on the quality of the initial solution. A high-quality initial solution can significantly reduce the computational effort required in subsequent search processes. Variable neighborhood search, with its diversified neighborhood search strategy, can quickly find a near-optimal initial solution, thus improving the overall efficiency of the algorithm (Hansen and Mladenović, 2001). In addition, the B&P algorithm needs to explore a vast search space to find the optimal solution. Variable neighborhood search, through dynamic adjustment of neighborhood structures, can conduct both broad and deep searches in different regions of the solution space, thus covering more potential optimal solution areas (Shao and Xin, 2019). In this problem, the need to select several ATTWs for large-scale vessels increases both the solution space and the complexity of the process. Therefore, the STFVNS algorithm is specifically designed to obtain a better initial scheme. The pseudocode for STFVNS is presented as Algorithm 3.

Algorithm 3 (Generate a better initial scheme)

Input:

The data of the scheduled vessels include draft, UKC, ETA, and $[ear^r, lat^r]$; $\underline{N}_{\bar{k}}(\bar{k} < \bar{k}_{max})$: Neighborhood structure for shaking;

$\underline{N}_{\bar{l}}(\bar{l} < \bar{l}_{max})$: Neighborhood structure for variable neighborhood descent.

Output:

\bar{S} : The optimal initial scheme

1 Function: Generate a better initial scheme.

2 for each vessel $i \in I$ do

3 if $d_i + UKC_i > Chart\ depth$ then

4 if $EAT < ear_i^r$ then

5 Scheduled time $\leftarrow ear_i^r$

6 else if $ear_i^r < ETA < lat_i^r$ then

7 Scheduled time $\leftarrow ETA$

8 end if

9 end if

10 end for

11 for each vessel $i^O \in I^O$ and $i^D \in I^D$ do

12 if the scheduled time of $i^O <$ the scheduled time of i^D then

13 The scheduled time of $i^O \leftarrow$ the last scheduled time of i^D

14 end if

15 end for

16 The initial scheme \bar{S} is obtained by arranging i according to the scheduled time from earliest to latest

17 While $\bar{k} < \bar{k}_{max}$ do

18 Shaking the \bar{S} uses $\underline{N}_{\bar{k}}$ to obtain the neighborhood scheme \bar{S}^*

19 The local optimal scheme \bar{S}^{**} is generated using variable neighborhood descent for \bar{S}^*

20 While $(\bar{l} < \bar{l}_{max})$ do

21 Perform $\underline{N}_{\bar{l}}$ on \bar{S}^* to obtain the local optimal scheme \bar{S}^{**}

22 if $f(\bar{S}^{**}) < f(\bar{S}^*)$ then

23 $\bar{S}^* \leftarrow \bar{S}^{**}$, $l \leftarrow 1$

24 else

25 $l = l + 1$

26 end if

27 end while

28 if $f(\bar{S}^*) < f(\bar{S})$ then

29 $\bar{S} \leftarrow \bar{S}^*$, $k \leftarrow 1$

30 else

31 $k = k + 1$

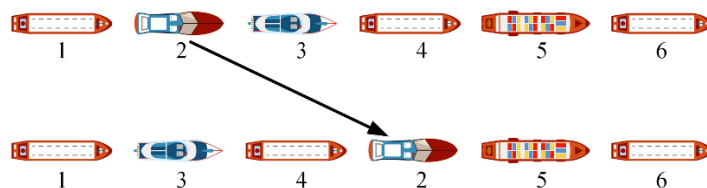
32 end if

33 end while

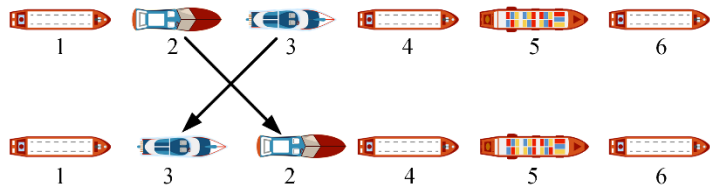
34 End function

35 Return the optimal scheme \bar{S}

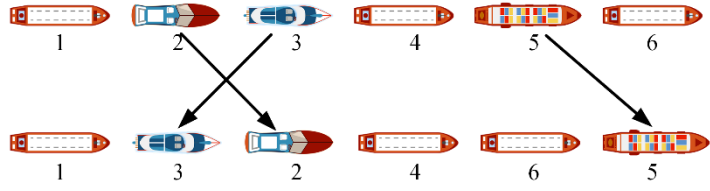
1 Nine neighborhood operators are employed in STFVNS, including three neighborhood operators within a
2 scheme (as shown in Fig. 4) and six neighborhood operators among schemes (as shown in Fig. 5). During STFVNS
3 execution, the neighborhood shakes six times, meaning that one of the six inter-scheme neighborhood operators is
4 randomly selected each time for the k th time. Variable neighborhood descent (VND) is executed 9 times, utilizing a
5 neighborhood structure that includes three neighborhood operators within a scheme and six neighborhood operators
6 among schemes.



(a) Randomly change the position of a vessel.

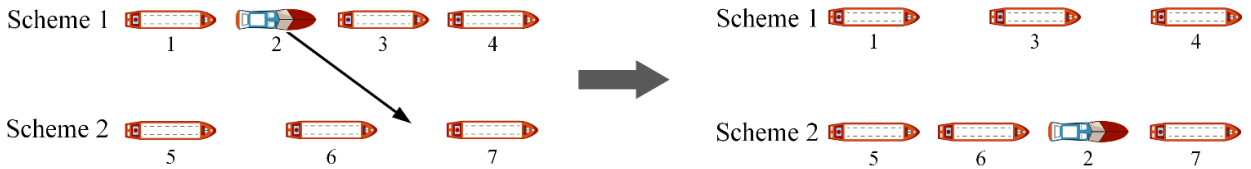


(b) Randomly exchange the positions of two vessels.

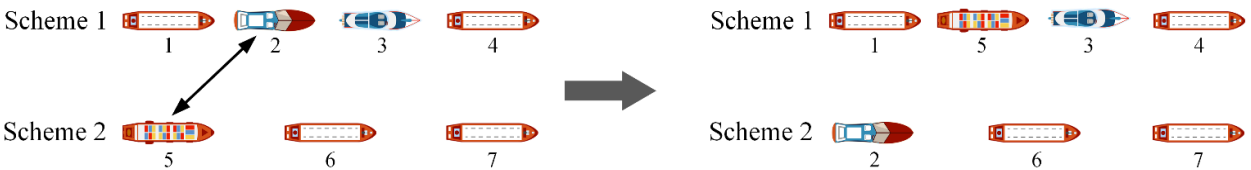


(c) Randomly exchange the positions of two vessels and change the position of a vessel.

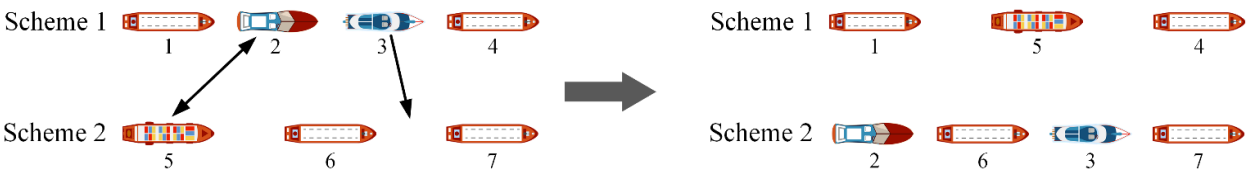
Fig. 4. The neighborhood operator within a scheme.



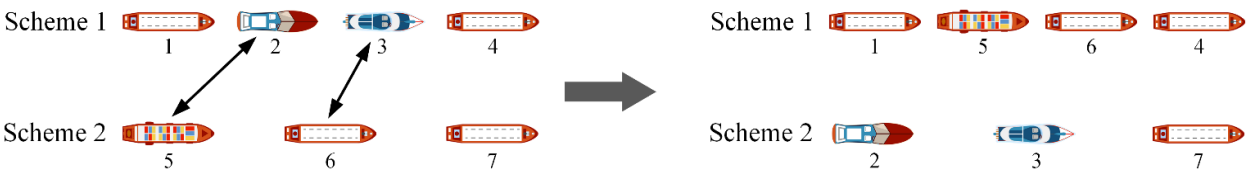
(a) Randomly change the position of a vessel.



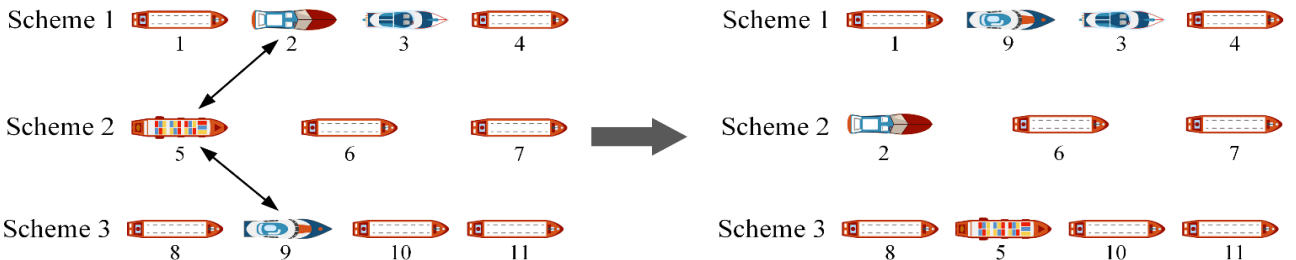
(b) Randomly exchange the positions of two vessels.



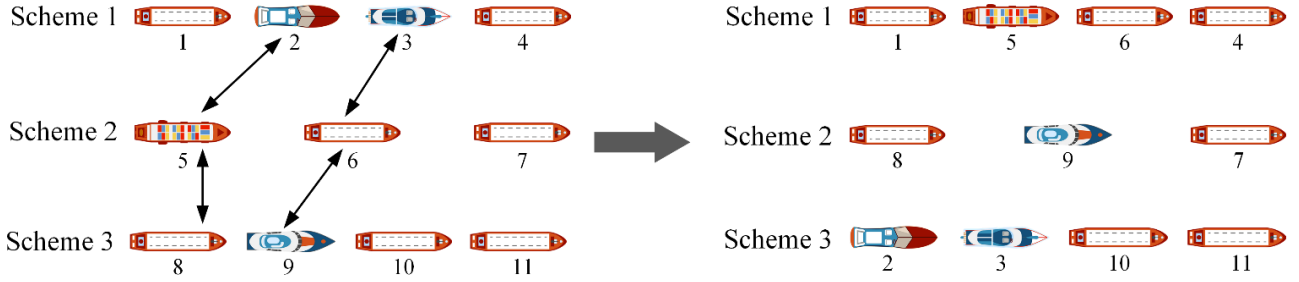
(c) Randomly exchange the positions of two vessels and change the position of a vessel.



(d) Randomly exchange the positions of two neighboring vessels.



(e) Randomly change the positions of three vessels.



(f) Randomly change the positions of two neighboring vessels.

Fig. 5. The neighborhood operator among schemes.

5.2.3. Improved label-setting algorithm for solving the subproblem

In this study, the pricing subproblem is essentially an NP-hard problem involving the determination of the optimal solution. Typically, it is solved using the label-setting algorithm based on dynamic programming (Shen et al., 2020). Therefore, an ILSA is proposed, including the definition of labels, extension rules, and dominance rules.

(1) Define the label

Each vessel schedule forms a label state, and different label states indicate different meanings. $B_i = (v(B_i), r(B_i), \bar{A}(B_i), \bar{c}(B_i), \mathbb{Q}(B_i), \mathbb{C}(B_i))$ represents any partial scheduling scheme from the first vessel that meets the scheduling requirements of the vessel i . The symbols in the label are defined as shown in Table 3.

Table 3

Definition of each element in the label.

Symbol	Meaning
$v(B_i) = i$	The last vessel scheduled for this part of the scheduling scheme
$r(B_i)$	The ATTW selected for the vessel i in this part of the scheduling scheme
$t(B_i)$	The earliest start time of the vessel i in this part of the scheduling scheme
$\bar{A}(B_i)$	A $ A_{2i} $ dimensional vector that labels the dangerous goods vessel, set to one if the vessel i is and to zero otherwise
$\bar{c}(B_i)$	The reduced cost of this part of the scheduling scheme
$\mathbb{Q}(B_i)$	The set of vessels scheduled and vessels that are not scheduled by the part of the scheduling scheme
$\mathbb{C}(B_i)$	The set of vessels scheduled immediately after the vessel i in this part of the scheduling scheme, i.e., a set of successively schedulable vessels

(2) Extension rules

The initial label is generated starting from the first vessel that satisfies the scheduling requirements, and then the new label is expanded by traversing the $\mathbb{C}(B)$ until the label cannot be expanded. The label of the vessel i is $B_i = (v(B_i), r(B_i), \bar{A}(B_i), \bar{c}(B_i), \mathbb{Q}(B_i), \mathbb{C}(B_i))$. The new label for the expansion of vessel j from $\mathbb{C}(B_i)$ that can be scheduled immediately after i is $B_j = (v(B_j), r(B_j), \bar{A}(B_j), \bar{c}(B_j), \mathbb{Q}(B_j), \mathbb{C}(B_j))$. The expansion rules are provided in Eqs. (32)-(38).

$$v(B_j) = j \quad (32)$$

$$r(B_j) = r \quad (33)$$

$$t(B_j) = \max\{t(B_i) + S_i, ear_j^{w_j}\} \quad (34)$$

$$\bar{A}(B_j) = \begin{cases} 1, & j \in A_2 \\ 0, & j \in A_1 \end{cases} \quad (35)$$

$$\bar{c}(B_j) = \bar{c}(B_i) + \bar{c}_{ij} \quad (36)$$

$$\mathbb{Q}(B_j) = \mathbb{Q}(B_i) \cup \{j\} \quad (37)$$

$$\mathbb{C}(B_j) = \mathbb{C}(B_i) - j - \{\bar{l}: (j, \bar{l}) \in A/t(B_j) + S_j + S_{\bar{l}} > lat_i^{r_l}\} \quad (38)$$

1 (3) Dominance rule

2 During the label expansion process, each vessel can be assigned multiple labels. As the number of vessels grows,
3 the number of labels also increases, resulting in a decrease in the operational speed of the label algorithm. We em-
4 power the label-setting algorithm with the ability to eliminate useless scheduling schemes using domination rules.
5 These rules help eliminate partial schemes that are unlikely to generate optimal scheduling schemes, thus reducing
6 the search space and improving the algorithm's efficiency. Assume the two labels of the scheduled vessel i are $B_i =$
7 $(v(B_i), r(B_i), \bar{A}(B_i), \bar{c}(B_i), \mathbb{Q}(B_i), \mathbb{C}(B_i))$ and $B_i^* = (v(B_i^*), r(B_i^*), \bar{A}(B_i^*), \bar{c}(B_i^*), \mathbb{Q}(B_i^*), \mathbb{C}(B_i^*))$, respectively.
8 When rules (39)-(42) are satisfied, consider that B_i dominates B_i^* . The label can be deleted in this situation.

$$t(B_i) \leq t(B_i^*) \quad (39)$$

$$\bar{c}(B_i) \leq \bar{c}(B_i^*) \quad (40)$$

$$\mathbb{Q}(B_i) \subseteq \mathbb{Q}(B_i^*) \quad (41)$$

$$\mathbb{C}(B_i) \subseteq \mathbb{C}(B_i^*) \quad (42)$$

9 By relaxing the dominance rule, the algorithm effectively reduces the number of labels in the set $\mathbb{C}(B)$. Since
10 each large vessel in the pricing subproblem has one or several ATTWs, the number of vessels in the $\mathbb{C}(B)$ increases
11 during label expansion, which, in turn, increases the number of labels. The surge in the number of labels affects the
12 efficiency of the column generation algorithm, so it is necessary to reduce the number of the immediately after vessels
13 in the $\mathbb{C}(B)$. The increase in total waiting costs resulting from adding these immediately after vessels to the schedul-
14 ing scheme is calculated. Then, half of the number of immediately-after vessels is retained in descending order,
15 reducing the total number of labels while retaining the labels that can find lower waiting costs schemes, and finally
16 accelerating column generation. This way accelerates column generation by reducing the total number of labels while
17 retaining the labels that correspond to lower waiting costs schemes.

18 5.2.4. Branching strategy based on original problem variables

19 If the variables in the RMP are branched directly, it necessitates the addition of new constraints to the RMP,
20 resulting in the introduction of new dual variables. This branching strategy can significantly disrupt the structure of
21 the subproblem, making programming and computation cumbersome for both the RMP and the subproblem. There-
22 fore, we adopt a strategy where the original problem variables are branched, and constraints are added to the sub-
23 problem. The specific steps are outlined below:

24 Step 1: After column generation, determine whether the optimal solution is an integer solution to the original
25 problem, and if not, find the first vessel containing a non-integer solution in the order of vessel number from smallest
26 to largest.

27 Step 2: Arrange f_{it} in order from early to late, choosing the first f_{it} that is not an integer. If $\sum_{a_i \in S_i} \mathbb{P}K_{a_i} = f_{it}$
28 is not an integer, then branch to the variable, including both $t' \leq t$ and $t' > t$ branches. The transformation rules
29 for the master problem and the subproblem are as follows: For $t' < t$, add $t' < t$ to the subproblem, e.g., let f_{it}
30 of $t' > t$ be zero, and delete the column containing $F_{a_i}^t$ of $t' < t$ that has been added to the master problem. In
31 the step, \mathbb{P} set to one if in scheme a_i , vessel i begins entering port at moment t and to zero otherwise.

32 Step 3: If all f_{it} are integers, arrange g_{it} , from the earliest to the latest according to moment t , select the first
33 g_{it} that is not an integer. If $\sum_{a_i \in S_i} \mathbb{Q}K_{a_i} = g_{it}$ is not an integer, it is divided into two branches $t' \leq t$ and $t' > t$.
34 Refer to step 2 for transforming the master problem and the subproblem. In the step, \mathbb{Q} set to one if in scheme a_i ,
35 vessel i begins leaving port at moment t and to zero otherwise.

36 5.2.5. Search strategy

37 Common search strategies include depth-first and breadth-first strategies (Xie, 2017). When the depth of the

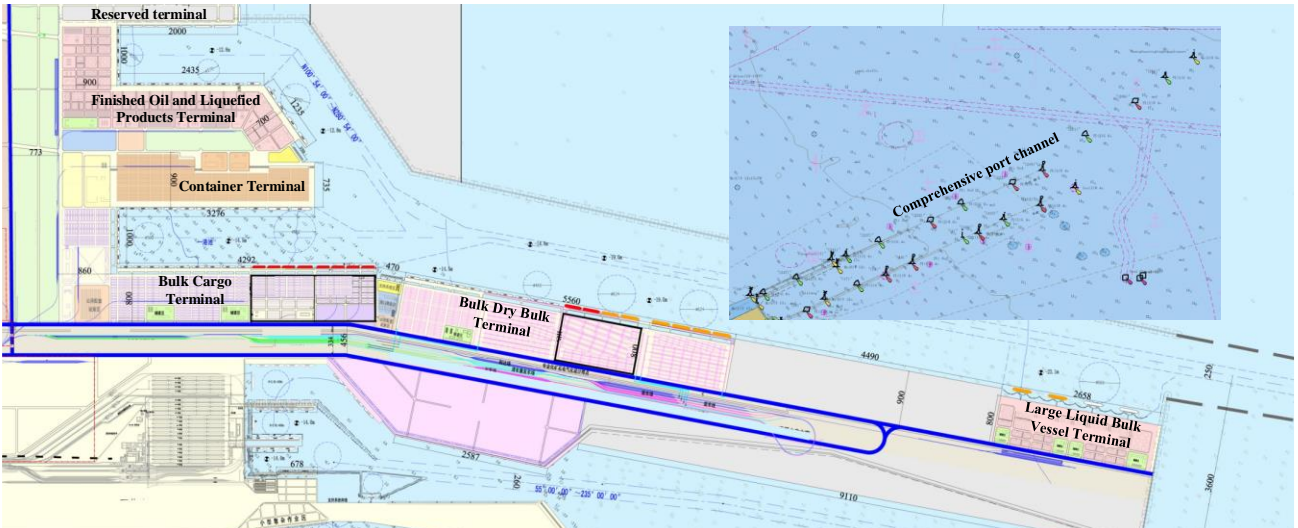
1 search tree is small, the depth-first search strategy can quickly find the problem’s upper bound value. However, due
 2 to the higher number of decision variables in this paper, which leads to more branches, using the depth-first strategy
 3 would result in a longer time to find the optimal solution. Therefore, this paper employs the breadth-first strategy.

4 6. Computational experiments

5 This section includes a series of comprehensive numerical experiments designed to validate the effectiveness of
 6 the proposed model and evaluate the efficiency of the algorithms employed. These algorithms are implemented using
 7 Python 3.9 and the CPLEX solver. The tests are run on a computer equipped with a 2.2GHz Intel(R) Core(TM) i7-
 8 10870H CPU and 16GB of RAM. To accommodate rescheduling needs while capturing current data, a computational
 9 time limit of 3600 seconds is set.

10 6.1. Introduction to the experimental area and generation of test instances

11 The experiments were conducted at Huanghua Port, a real-world multi-functional port. Fig.6 displays the port’s
 12 physical layout, featuring berths for bulk cargo, containers, oil, and LNG. The largest berth can accommodate
 13 200,000-ton bulk carriers and 20,000 TEU container vessels. The port’s channel stretches for 32 nautical miles. To
 14 facilitate safe navigation, a one-way traffic pattern is implemented for vessels in the channel, where the speed of
 15 vessels significantly varies during the entry and exit processes (Zhang et al., 2022).



16
 17 **Fig.6.** The physical layout of Huanghua Port.

18 The vessel dataset utilized in our computational experiments is generated using randomization techniques. Let
 19 $R\bar{U}(N^{lb}, N^{ub})$ denote that the random number R follows a uniform distribution of $Uniform(N^{lb}, N^{ub})$. Both the
 20 arrival and estimated departure times of each vessel i can be represented by $ARR_i\bar{U}(0.72)$ and $ETD_i\bar{U}(0.72)$,
 21 measured in time steps, respectively. In this example, we generated instances at three different scales: low traffic flow
 22 with $[10, 25)$ vessels, medium traffic flow with $[25, 35)$ vessels, and heavy traffic flow with $[35, 50)$ vessels. For
 23 each scale, we created 9 sets of instances, each with varying traffic densities, resulting in a total of 27 sets. The
 24 numbers of inbound and outbound vessels for these scales are $\{5, 9, 12\}$, $\{13, 15, 17\}$, and $\{18, 20, 24\}$, respectively.
 25 In each set, 5 test instances were randomly generated, totaling 135 instances. To illustrate, a heavy traffic flow group
 26 with 20 inbound and 18 outbound vessels is labeled as “H_20_18”. Furthermore, the proportion of large-scale and
 27 dangerous goods vessels is set at 20% and 10%, respectively. A safety slot of 10 minutes is maintained between
 28 vessels. Other maritime data used in the experiments were sourced through applications to government departments
 29 and downloads from official websites, as detailed in Table 4.

1 **Table 4**

2 Experimental data description.

Data type	Source	Time Range
AIS data	https://www.hifleet.com/	2/1/2021-3/1/2023
Official Electronic Chart Data (S-57)	http://www.enclive.cn/	2/1/2022
Tidal data of Huanghua Port	http://www.soa.gov.cn/	2/1/2021-3/20/2023
Vessel actual scheduling data of the long channel	http://www.czgwjt.com/view/index.aspx	3/11/2023-3/13/2023

3 *6.2. Comparison of the ATTWs of large-scale vessels*

4 The PSRT method was utilized to calculate the ATTWs for large-scale vessels with drafts of 18.0 m, 18.3 m,
5 18.6 m, and 19.0 m, covering the period from July 1, 2022, to December 31, 2022. These calculations were then
6 compared with the results from the single-point ride-tide calculation as specified in the “Port Infrastructure Maintenance
7 Regulations” (MOT, 2023). The results of these calculations are presented in Table 5, and the duration comparison
8 is illustrated in Fig.7.

9 **Table 5**

10 ATTWs results of the PSRT method and the single-point ride-tide method.

Draft (m)	ATTWs by the PSRT method			ATTWs by the single-point ride-tide method		
	Start time	End time	Duration (min)	Start time	End time	Duration (min)
18.0	00:00 7/1	04:45 7/1	285	00:00 7/1	04:35 7/1	275
	13:35 7/1	23:59 7/1	624	14:06 7/1	23:59 7/1	593
	00:00 7/2	05:19 7/2	319	00:00 7/2	05:10 7/2	310
	14:06 7/2	23:59 7/2	593	14:35 7/2	23:59 7/2	564
18.3	00:00 7/1	04:02 7/1	242	00:34 7/1	03:57 7/1	203
	14:21 7/1	23:59 7/1	578	15:03 7/1	19:12 7/1	249
	00:00 7/2	04:37 7/2	277	01:13 7/2	04:28 7/2	195
	14:53 7/2	23:59 7/2	546	15:33 7/2	19:29 7/2	236
18.6	00:54 7/1	03:24 7/1	150			
	15:09 7/1	19:12 7/1	243	16:23 7/1	17:42 7/1	79
	20:00 7/1	20:22 7/1	22			
	01:25 7/2	03:58 7/2	153			
	15:42 7/2	19:25 7/2	223	16:52 7/2	17:57 7/2	65
19.0	16:33 7/1	17:13 7/1	40	Failure to ride-tide		0
	17:08 7/2	17:37 7/2	29	Failure to ride-tide		0
	17:39 7/3	18:00 7/3	21	Failure to ride-tide		0

11 Note: Due to the space limitation, only some results are listed here.

12 The computational results reveal a marked improvement in the calculated ATTWs for vessels with drafts of 18
13 meters and 18.3 meters when using the PSRT method, compared to the single-point ride-tide method. This enhance-
14 ment significantly broadens the options for tidal entry and exit for larger vessels, underscoring the PSRT method’s
15 potential in optimizing tidal scheduling. For vessels with a draft of 18.6 meters, the single-point ride-tide method
16 typically offers only a limited ATTW each day. In contrast, the PSRT method considerably extends the ATTWs,
17 providing two to three ATTWs on certain dates, thus markedly increasing scheduling flexibility for vessels. Regarding
18 vessels with a draft of 19 meters, the single-point tide-ride method fails to provide any ATTWs, preventing them from
19 berthing at the port. However, the effective use of tidal resources via the PSRT method has successfully created usable
20 ATTWs, allowing the channel to accommodate vessels with a draft of 19 meters or more. This enhancement can
21 significantly increase the port’s capacity.

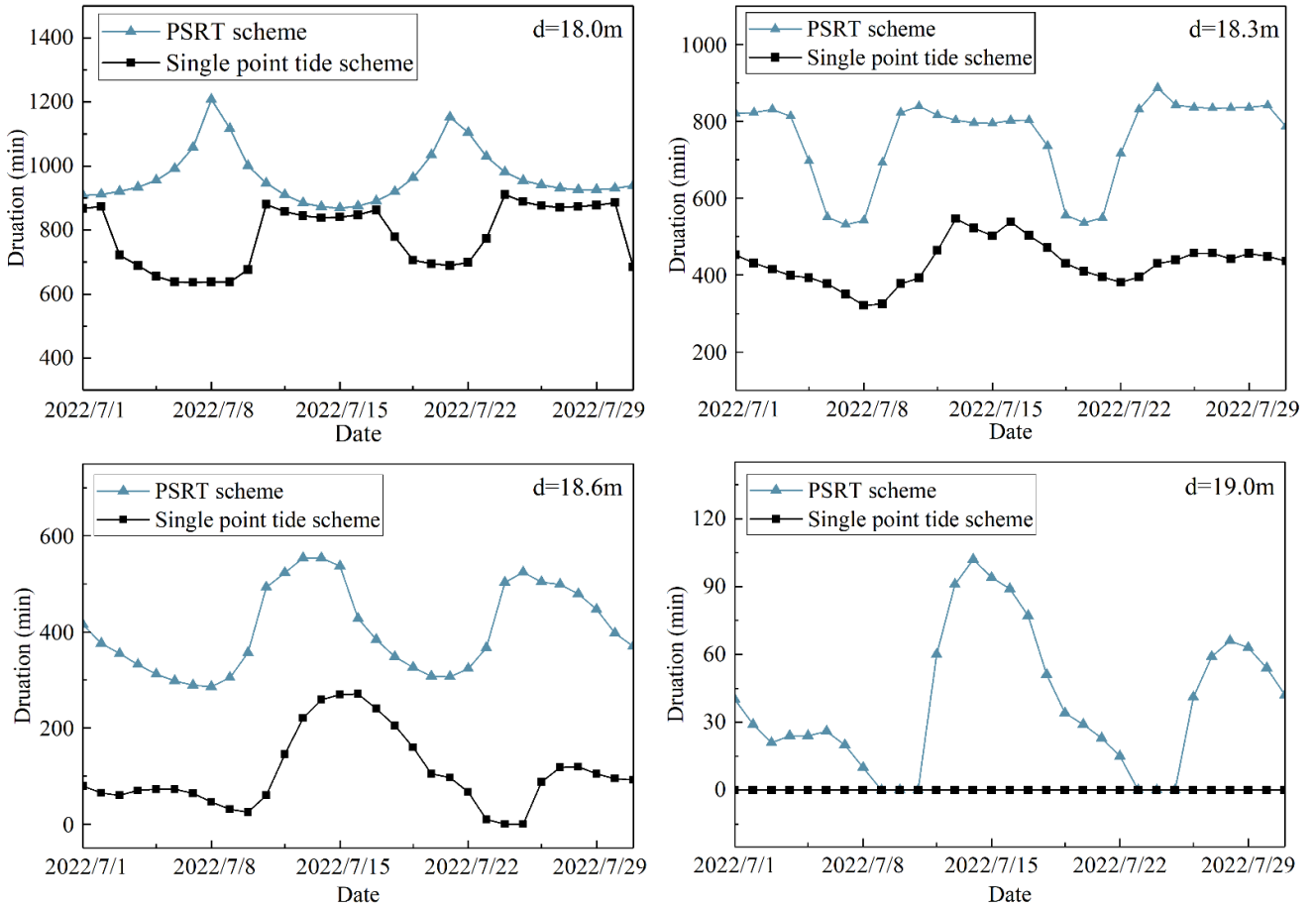


Fig. 7. Comparison of available tidal time windows (ATTWs).

6.3. Validation of the efficacy of the algorithm

6.3.1. Benchmark methods

To assess the efficacy of the improved B&P algorithm in terms of solution quality and computational time, this section employs three benchmark methods and compares them to the newly proposed algorithm using instances of varying sizes. This evaluation facilitates an assessment of our algorithm's performance against established benchmarks. The first benchmark method involves solving the model directly using the branch-and-bound algorithm integrated into the CPLEX. The second benchmark method utilized is CG, a well-established approach for addressing combinatorial optimization problems, especially elementary shortest-path problems with resource constraints. The third benchmark method is an improved genetic algorithm (IGA), which employs Q-learning to adaptively modify crossover and mutation parameters in the genetic algorithm, thereby enhancing the algorithm's search capabilities (Zhang et al., 2022).

6.3.2. Comparison with CPLEX, CG, and IGA methods

This subsection employs the proposed improved B&P algorithm, along with three benchmark methods, to solve the instances. Table 6 compares the performance of the improved B&P algorithm with that of the CPLEX, CG, and IGA methods across 27 groups, encompassing a total of 135 tested instances. The average objective value of the optimal solution, highlighted in bold font, is considered applicable only when all five instances in a group simultaneously achieve optimality. Further details on the computational results for each instance group are available in Appendix A.

1 **Table 6**

2 Comparison results of improved B&P with the CPLEX, CG, and IGA methods.

Group	Instance	Improved B&P			CG			CPLEX			IGA		Gap (%)
		LB (million)	Obj (million)	Time (s)	LB (million)	Obj (million)	Time (s)	LB (million)	Obj (million)	Time (s)	Obj (million)	Time (s)	
Low traffic flow													
L_5_5	5	0.115	0.117	5.17	0.115	0.117	5.94	0.117	0.117	16.42	0.138	4.43	0.00
L_5_9	5	0.124	0.126	5.88	0.123	0.126	7.16	0.126	0.126	16.80	0.157	4.70	0.00
L_5_12	5	0.121	0.123	6.62	0.121	0.124	7.27	0.123	0.123	18.19	0.135	5.00	0.00
L_9_5	5	0.120	0.124	7.60	0.120	0.126	9.32	0.124	0.124	16.32	0.142	5.40	0.00
L_9_9	5	0.126	0.127	7.16	0.126	0.130	8.48	0.127	0.127	17.35	0.159	5.23	0.00
L_9_12	5	0.137	0.141	8.06	0.137	0.143	9.28	0.141	0.141	18.84	0.163	5.57	0.00
L_12_5	5	0.158	0.159	7.33	0.158	0.162	9.01	0.159	0.159	19.91	0.185	5.29	0.00
L_12_9	5	0.158	0.159	9.94	0.158	0.162	11.03	0.159	0.159	21.42	0.185	6.15	0.00
L_12_12	5	0.168	0.170	10.58	0.168	0.173	12.14	0.170	0.170	22.49	0.193	6.56	0.00
Average												0.00	
Medium traffic flow													
M_13_13	5	0.301	0.322	18.87	0.301	0.398	33.38	0.322	0.322	109.91	0.357	15.97	0.00
M_13_15	5	0.325	0.344	23.79	0.325	0.426	41.91	0.344	0.344	130.40	0.382	20.19	0.00
M_13_17	5	0.318	0.339	25.23	0.319	0.419	44.52	0.339	0.339	136.55	0.375	21.45	0.00
M_15_13	5	0.315	0.340	30.52	0.315	0.420	53.64	0.340	0.340	158.50	0.377	25.99	0.00
M_15_15	5	0.331	0.347	28.48	0.331	0.430	50.17	0.347	0.347	150.16	0.385	24.28	0.00
M_15_17	5	0.361	0.386	32.44	0.361	0.478	56.99	0.386	0.386	166.51	0.427	27.65	0.00
M_17_13	5	0.415	0.436	30.64	0.415	0.540	53.89	0.436	0.436	159.04	0.482	26.06	0.00
M_17_15	5	0.415	0.437	37.78	0.415	0.542	66.24	0.437	0.437	188.73	0.483	32.19	0.00
M_17_17	5	0.442	0.467	41.57	0.442	0.579	72.79	0.467	0.467	204.45	0.516	35.44	0.00
Average												0.00	
Heavy traffic flow													
H_18_18	5	0.588	0.691	76.34	0.599	0.775	252.51	0.613	0.639	846.92	0.866	66.84	7.53
H_18_20	5	0.634	0.729	95.29	0.634	0.828	309.35	0.648	0.675	1051.06	0.930	79.90	7.41
H_18_24	5	0.625	0.733	101.01	0.625	0.818	326.48	0.633	0.666	1112.52	0.917	83.87	9.14
H_20_18	5	0.627	0.735	121.32	0.627	0.820	387.40	0.635	0.668	1331.12	0.920	97.84	9.12
H_20_20	5	0.639	0.748	113.59	0.639	0.833	364.26	0.647	0.680	1248.13	0.936	92.52	9.09
H_20_24	5	0.700	0.816	128.70	0.700	0.902	409.60	0.715	0.742	1410.89	1.019	102.96	9.07
H_24_18	5	0.778	0.903	121.81	0.778	0.992	388.88	0.787	0.824	1336.50	1.127	98.18	8.75
H_24_20	5	0.780	0.905	149.29	0.780	0.994	471.25	0.796	0.826	1632.15	1.129	117.09	8.73
H_24_24	5	0.827	0.957	163.80	0.827	1.048	514.85	0.836	0.874	1788.61	1.193	127.13	8.67
Average												8.61	

3 As shown in Table 6, the improved B&P algorithm demonstrates the highest solution quality. In terms of com-
4 putation time, both the improved B&P algorithm and CG significantly outperform CPLEX. In contrast, the improved
5 B&P algorithm exhibits significantly greater computational speed than the CPLEX solver, often achieving a notable
6 difference of several times. For instance, in the instance scale “H_24_20”, the improved B&P algorithm is over 10
7 times faster than CPLEX (149.29 s versus 1632.15 s). This advantage can be attributed to the additional computational
8 time CPLEX requires to incorporate new dual variables into the MP. This result demonstrates that the improved B&P
9 algorithm effectively addresses the challenges of ride-tide planning and vessel scheduling problems. Compared to
10 the IGA, the improved B&P algorithm exhibits similar computation times for low and medium traffic flows. This
11 efficiency is due to the improved B&P algorithm operating on a fixed number of high-quality columns, as opposed
12 to exhaustively considering all possible schemes, leading to fast convergence. In scenarios with heavy traffic flow,
13 the computation time of the improved B&P algorithm is marginally longer than that of the IGA. However, the im-
14 proved B&P algorithm achieves significantly lower objective values than the IGA.

15 Table 6 further shows that our algorithm achieves an average gap of 0 between the actual objective value and
16 the optimal lower bound in instances with low and medium traffic flow. Even in heavy traffic flow situations, this
17 gap is just 8.61%, underscoring the exceptional accuracy of our algorithm. For low and medium traffic flow instances,
18 our algorithm consistently resolves problems within 40 seconds. In heavy traffic scenarios, resolutions are achieved
19 in less than 170 seconds. However, the computation time of CPLEX for solving low, medium, and heavy traffic flows

is 18.64, 156.03, and 1306.43 seconds, respectively. As the vessel schedule is updated quite often in the real world, the operator requires the decision to be updated within just a few minutes (less than 3 minutes). It can be seen that the computational efficiency of CPLEX cannot meet the actual needs. This blend of rapid computation and high-quality solutions underscores the effectiveness of the proposed improved B&P algorithm.

6.3.3. Comparison with original B&P algorithm

To evaluate the effectiveness of the improved B&P algorithm on problems of different scales, this subsection compares the improved B&P algorithm with the original B&P algorithm, focusing on their performance in terms of solution quality and computation time. Each set of experiments is conducted five times, and the average results are reported. Table 7 presents the experimental results of the two algorithms under low, medium, and heavy traffic flow scenarios. For ease of comparison, the superior results are highlighted in bold.

Table 7

Comparison results of improved B&P with the original B&P.

Group	Instance	Improved B&P		Original B&P	
		Obj (million)	Time (s)	Obj (million)	Time (s)
Low traffic flow					
L_5_5	5	0.117	5.17	0.117	210.62
L_5_9	5	0.126	5.88	0.126	238.21
L_5_12	5	0.123	6.62	0.123	267.48
L_9_5	5	0.124	7.60	0.124	306.82
L_9_9	5	0.127	7.16	0.127	290.05
L_9_12	5	0.141	8.06	0.141	325.16
L_12_5	5	0.159	7.33	0.159	295.90
L_12_9	5	0.159	9.94	0.159	381.98
L_12_12	5	0.170	10.58	0.170	427.07
Medium traffic flow					
M_13_13	5	0.322	18.87	0.322	355.75
M_13_15	5	0.344	23.79	0.344	448.47
M_13_17	5	0.339	25.23	0.339	476.35
M_15_13	5	0.340	30.52	0.340	575.60
M_15_15	5	0.347	28.48	0.347	537.95
M_15_17	5	0.386	32.44	0.386	611.82
M_17_13	5	0.436	30.64	0.436	578.04
M_17_15	5	0.437	37.78	0.428	712.29
M_17_17	5	0.467	41.57	0.479	783.27
Heavy traffic flow					
H_18_18	5	0.691	76.34	0.691	1196.65
H_18_20	5	0.729	95.29	0.802	1493.72
H_18_24	5	0.733	101.01	0.733	1583.13
H_20_18	5	0.735	121.32	0.809	1901.20
H_20_20	5	0.748	113.59	0.823	1780.43
H_20_24	5	0.816	128.70	0.896	2017.24
H_24_18	5	0.903	121.81	0.990	1908.97
H_24_20	5	0.905	149.29	0.992	3032.89
H_24_24	5	0.957	163.80	1.049	3205.55

From Table 7, it can be observed that in terms of solution quality, the improved B&P algorithm performs comparably to the original B&P algorithm in low and medium traffic flow scenarios. In the heavy traffic flow scenario, the improved B&P algorithm outperforms the original B&P algorithm in solution quality. Regarding computation time, the improved B&P algorithm is superior to the original algorithm in low, medium, and heavy traffic flow scenarios. The reasons mainly include:

i) The STFVNS is effective at finding high-quality initial solutions by systematically exploring different neighborhoods. This leads to better starting points for the B&P, which can significantly improve the overall solution quality. With better initial solutions, the B&P can converge more quickly to the optimal or near-optimal solutions, reducing the total computation time.

1 ii) The improved label-setting uses the optimal solution of the previous step to construct the current step's opti-
 2 mal solution. This recursive characteristic enables the algorithm to efficiently manage and store intermediate results,
 3 avoiding redundant computations.

4 iii) The original problem branching strategy helps effectively navigate the solution space, ensuring that the most
 5 promising branches are explored first, leading to faster identification of better solutions.

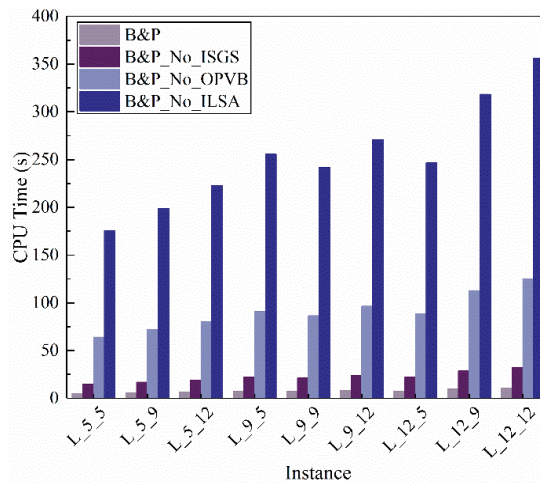
6 6.3.4. Comparison with different enhanced methods

7 In this subsection, the improved B&P algorithm along with three enhanced methods is utilized to solve the
 8 relevant problem instances. To simplify the presentation, the following notations are given:

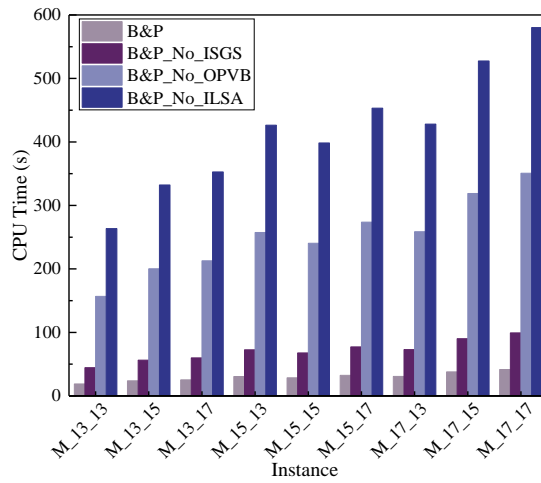
- 9 • B&P: The proposed improved B&P algorithm with all enhancement methods;
- 10 • B&P_No_ISGS: The improved B&P without initial scheme generation strategy (ISGS);
- 11 • B&P_No_ILSA: The improved B&P without improved label-setting algorithm (ILSA) where the common
 12 label-setting algorithm solves the subproblem;
- 13 • B&P_No_OPVB: The improved B&P without original problem variables is branched (OPVB).

14 Fig. 8 presents an overview of the impact of incorporating various enhanced methods on the performance of the
 15 improved B&P algorithm, where (a) to (c) denotes the comparison of the average solution times of different enhanced
 16 methods for the three traffic scenarios, respectively. Detailed computational results for each group of instances are
 17 available in Appendix B.

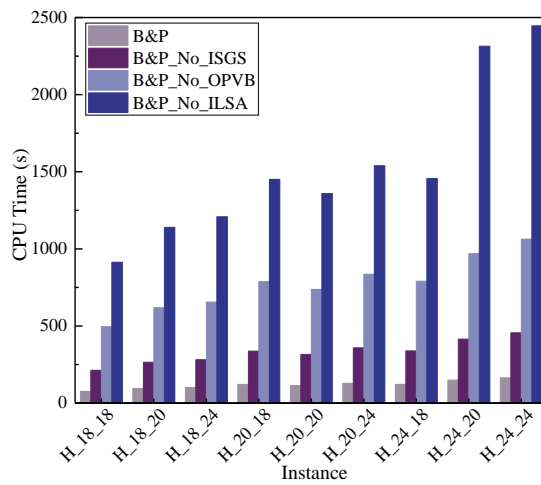
18 Through our experiments, we determined that several proposed enhancement methods significantly boost the
 19 algorithm's performance. The B&P_No_ILSA requires the most computational time. This is attributed to the im-
 20 proved label-setting algorithm, which notably reduces the number of calls to the label-setting algorithm and thus
 21 accelerates the resolution of the pricing subproblem. The B&P_No_OPVB shows medium computational time. In
 22 this method, original problem variables are branched without the need to add a new dual variable, involving only the
 23 corresponding constraint of the currently branched vessel. This strategy, which adds just one constraint per branch,
 24 is straightforward to implement and ensures that no solutions are overlooked during branching. While the
 25 B&P_No_ISGS achieves the same objective value as the B&P, its initial stage in the RMP involves low-quality
 26 columns that do not offer useful dual information. This leads to the inclusion of irrelevant columns, resulting in
 27 additional iterations.



28 (a) Benefits of different enhancement methods in low traffic flow.
 29



(b) Benefits of different enhancement methods in medium traffic flow.

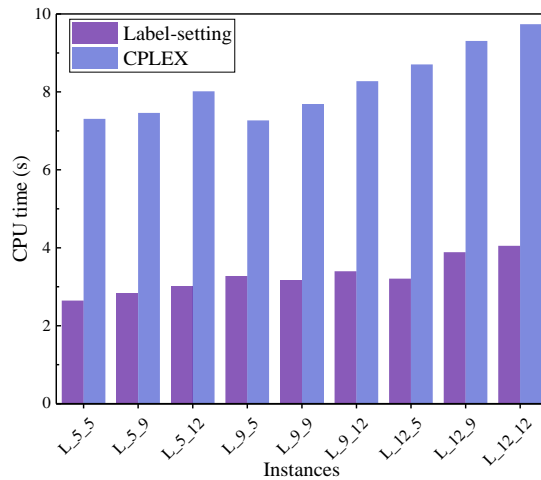


(c) Benefits of different enhancement methods in heavy traffic flow.

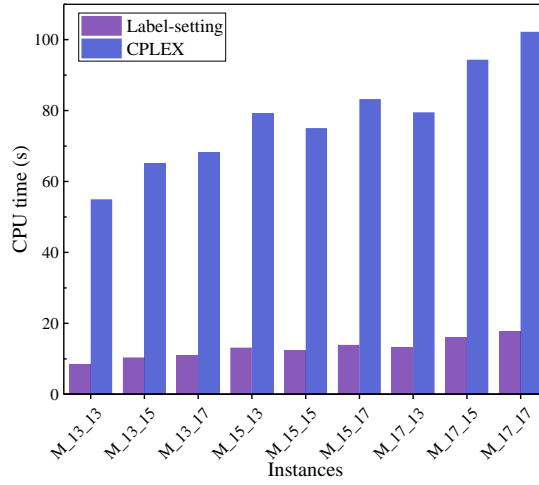
Fig. 8. Benefits of different enhancement methods in different traffic flow

6.3.5 Comparison of efficiency of solving subproblems

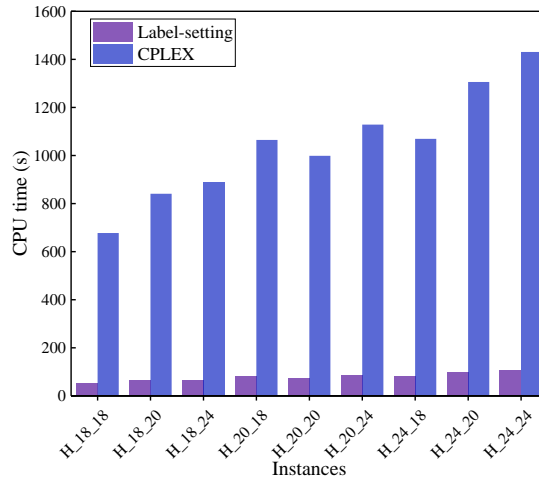
To verify the efficiency of the proposed improved label-setting algorithm (ILSA) in solving the pricing subproblem, this subsection compares the ILSA with CPLEX, focusing on their performance in terms of computation time. Each set of experiments is conducted five times, and the average results are reported. Fig. 9 presents the experimental results of the two methods in solving the pricing subproblem in low, medium, and heavy traffic flow scenarios.



(a) Comparison of the results of the two methods for solving sub-problems in low traffic flow.



(b) Comparison of the results of the two methods for solving sub-problems in medium traffic flow.

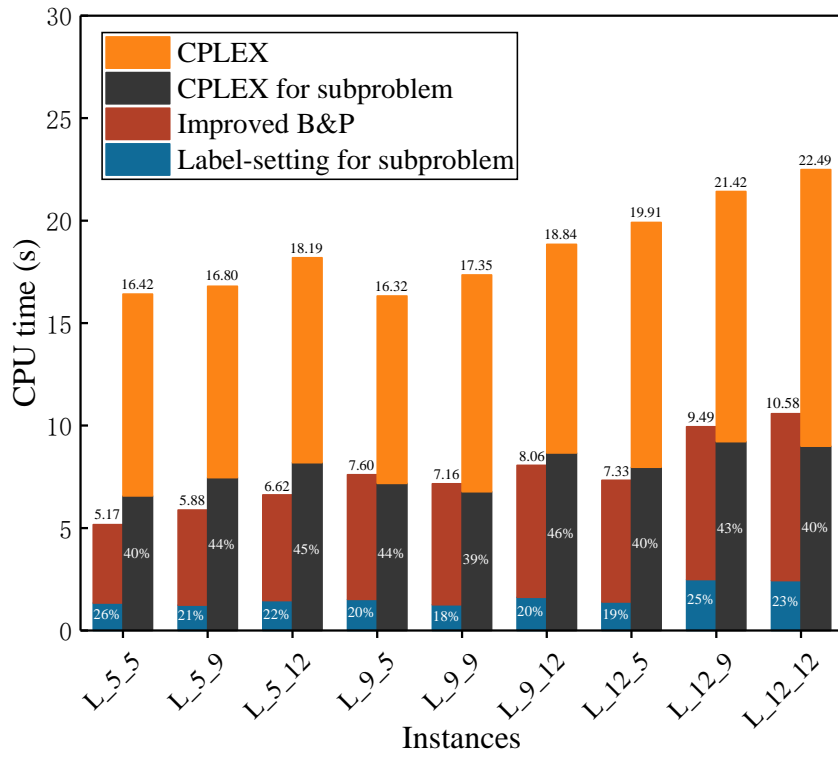


(c) Comparison of the results of the two methods for solving sub-problems in heavy traffic flow.

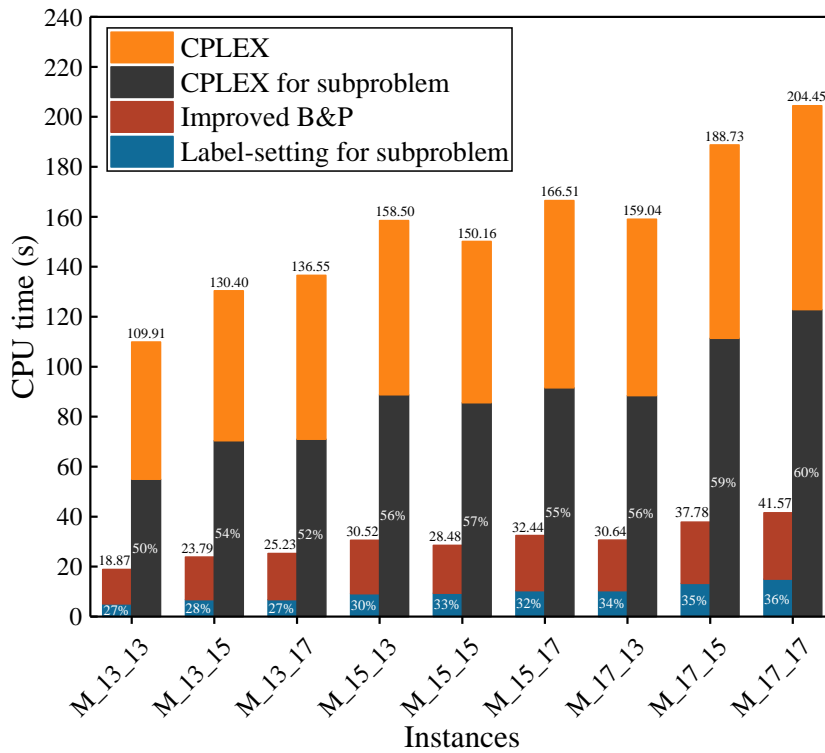
Fig. 9. Comparison of the results of the two methods for solving sub-problems in different traffic flow scenarios.

As shown in Fig. 9, the ILSA proposed in this paper outperforms CPLEX in solving subproblems in low, medium, and heavy traffic flow scenarios. This is because the ILSA can identify all columns with negative reduced costs. By selecting and adding several columns with the most negatively reduced costs to the current RMP, the number of iterations in the column generation algorithm can be reduced, thereby shortening the subproblem solving time. However, it is important to note that this method increases the size of the RMP. In the future, we will further explore how to effectively control the size of the RMP while reducing the number of iterations in the column generation algorithm.

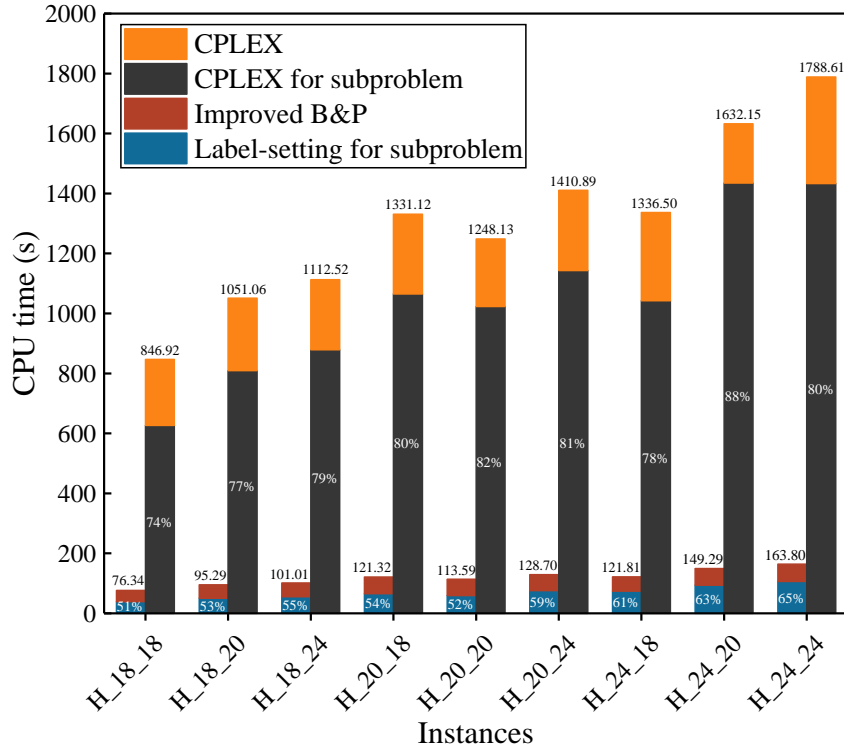
Fig. 10 shows the proportion of computation time spent on solving subproblems using two different methods relative to the total solution time. Under different traffic flow scenarios, the proportion of computation time spent on solving subproblems using the ILSA is always less than that of CPLEX, which also confirms the superiority of the proposed algorithm. Moreover, as the complexity of traffic flow scenarios increases, the proportion of computation time spent on solving subproblems using the ILSA gradually increases. This phenomenon can be attributed to the fact that as the problem size increases, the complexity of the subproblems also increases. For the ILSA, this may require handling more labels and performing more state transitions and updates, increasing the time required to solve each subproblem.



(a) In low traffic flow.



(b) In medium traffic flow.



(c) In heavy traffic flow.

Fig. 10. The proportion of computation time spent on solving subproblems using two different methods relative to the total solution time in different traffic flow scenarios.

6.3.6. Comparison with the current real-world scheme

To further validate the effectiveness of the proposed decision method, the new solution results are compared with those of the real-world scheme. At Huanghua Port, a minimum safe navigation time slot of 30 minutes is mandated between dangerous goods vessels and other vessel types. For two dangerous goods vessels, this time slot increases to 60 minutes, while it's only 10 minutes between two non-dangerous goods vessels. To prevent overtaking, faster container vessels must be dispatched at least 30 minutes after bulk carriers start entering the port. Table 8 provides a summary of key details and current real-world scheduling data (following the First-Come-First-Serve rule) for 13 vessels, including both bulk carriers and container vessels. Of these, vessels 1 to 4 are outbound, while vessels 5 to 13 are inbound. Importantly, vessels 10 and 12 require synchronization with tidal conditions for port entry. The vessel scheduling arrangement achieved using the methodology described in this paper is detailed in Table 9. The comparative results between the two approaches are illustrated in Figs. 11 and 12.

Table 8

The current real scheduling scheme for 13 vessels (FCFS).

Vessel's number	In or out	Berth's number	Draft (m)	Arrival or completion time	Actual in or out time	Waiting time (min)	Unit waiting cost (CNY)	Vessel's types	Ride tide	ATTWs
1	Out	5#	6.20	15:30 3/12	16:40 3/12	70	80	bulk	No	--
2	Out	4#	8.60	15:30 3/12	17:20 3/12	110	150	container	No	--
3	Out	HG4#	10.68	15:30 3/12	17:30 3/12	120	120	bulk	No	--
4	Out	K01	11.90	16:30 3/12	17:40 3/12	70	120	bulk	No	--
5	In	HG1#	4.70	12:00 3/12	12:20 3/12	20	100	bulk	No	--
6	In	8#	4.90	12:00 3/12	13:00 3/12	60	160	container	No	--
7	In	HG2#	10.40	12:00 3/12	13:10 3/12	70	140	bulk	No	--
8	In	7#west	5.50	12:00 3/12	13:50 3/12	110	160	container	No	--
9	In	6#	11.90	16:30 3/12	21:10 3/12	280	140	bulk	No	--
10	In	K02	18.42	16:35 3/12	08:34 3/13	959	200	bulk	Yes	08:34-08:59 3/13

1 *Continued*

Ves- sel's number	In or out	Berth's number	Draft (m)	Arrival or comple- tion time	Actual or out time	in time (min)	Waiting time	Unit wait- ing cost (CNY)	Vessel's types	Ride tide	ATTWs
11	In	7#east	7.2	18:00 3/12	21:50 3/12	230		160	container	No	--
12	In	K04	18.20	18:00 3/12	08:44 3/13	884		200	bulk	Yes	06:56-08:45 3/12 07:25-09:33 3/13
13	In	HG4#	12.85	18:30 3/12	22:00 3/12	210		140	bulk	No	--

2 **Table 9**

3 Optimized scheduling scheme for 13 vessels by improved B&P.

Ves- sel's num- ber	In or out	Berth's number	Draft (m)	Arrival or comple- tion time	Actual or out time	in time (min)	Waiting time	Unit wait- ing cost (CNY)	Vessel's types	Ride tide	ATTWs
1	Out	5#	6.20	15:30 3/12	22:08 3/12	398		80	bulk	No	--
2	Out	4#	8.60	15:30 3/12	21:58 3/12	388		150	container	No	--
3	Out	HG4#	10.68	15:30 3/12	22:18 3/12	408		120	bulk	No	--
4	Out	K01	11.90	16:30 3/12	22:28 3/12	358		120	bulk	No	--
5	In	HG1#	4.70	12:00 3/12	12:20 3/12	20		100	bulk	No	--
6	In	8#	4.90	12:00 3/12	12:00 3/12	0		160	container	No	--
7	In	HG2#	10.40	12:00 3/12	12:30 3/12	30		140	bulk	No	--
8	In	7#west	5.50	12:00 3/12	12:10 3/12	10		160	container	No	--
9	In	6#	11.90	16:30 3/12	16:30 3/12	0		140	bulk	No	--
10	In	K02	18.42	16:35 3/12	16:40 3/12	5		200	bulk	Yes	03:49-05:11 3/12 16:32-17:55 3/12
11	In	7#east	7.2	18:00 3/12	18:00 3/12	0		160	container	No	--
12	In	K04	18.20	18:00 3/12	18:28 3/12	28		200	bulk	Yes	03:08-05:37 3/12 15:52-18:28 3/12
13	In	HG4#	12.85	18:30 3/12	18:38 3/12	8		140	bulk	No	--

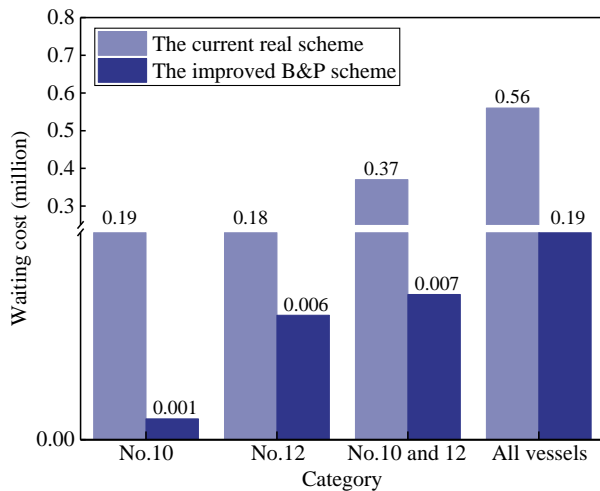


Fig. 11. Waiting costs comparison results.

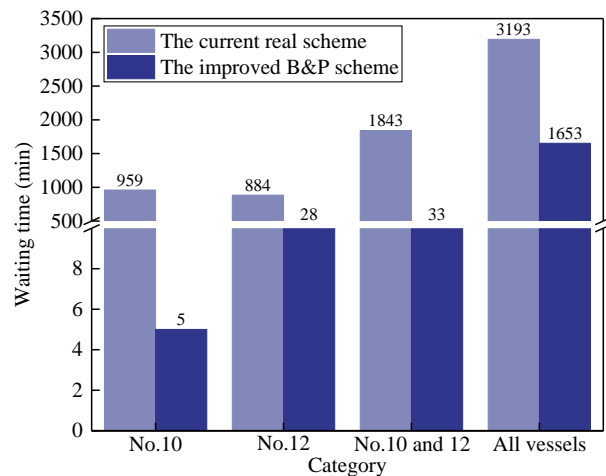


Fig. 12. Waiting time comparison results.

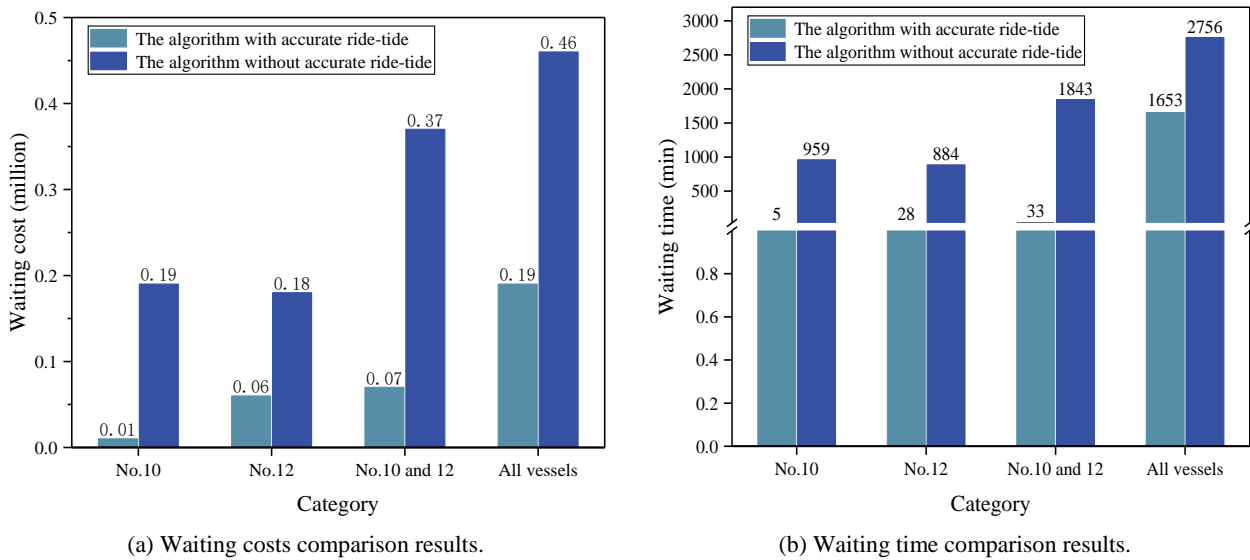
4 Comparing Tables 8 and 9, it is evident that in the current real-world scheme, vessel No. 10 lacked ATTWs on
5 March 12th, resulting in a postponed entry to March 13th. Similarly, while vessel No. 12 had an ATTW on the sched-
6 ulated entry date, it did not align with the planned entry time, preventing its port entry on March 12th. As illustrated in
7 Figs. 11 and 12, these delays for only two vessels, Nos. 10 and 12, led to a staggering waiting costs of 0.37 million.
8 The adoption of the PSRT method significantly optimized the vessels' ATTWs, enabling vessels Nos. 10 and 12 to
9 smoothly complete their planned entries on their arrival day. Compared to the current real-world scheme, the solution
10 derived from our model and algorithm reduced the waiting time for these large vessels by 1810 minutes, achieving a
11 waiting costs saving of 0.36 million.

12 Moreover, the scheme organizes the sequence of vessels entering and leaving the port during identical planned
13 times based on their navigation speed. For instance, vessels 5-8 have the same planned arrival time. Given the faster

1 navigation speed of container vessels compared to bulk carriers, prioritizing the entry of container vessels is prefer-
 2 able to minimize unnecessary waiting caused by overtaking in the long channel. This approach significantly improves
 3 the efficiency of vessel scheduling. The calculations show that while the actual solution incurred a total waiting cost of
 4 of 0.56 million, the scheme developed through our model and algorithm resulted in much lower waiting costs of only
 5 0.20 million.

6.3.7. Comparison with the method that does not consider accurate ride-tide

7 In order to assess the impact of incorporating accurate ride-tide on the overall performance of the algorithm,
 8 comparative computational experiments were conducted. The experiments compare the results of the algorithms that
 9 account for accurate ride-tide with those that do not. The experimental data for this comparison are derived from the
 10 actual data set presented in Section 6.3.6. The comparison results are illustrated in Fig. 13, which presents two key
 11 metrics: waiting costs and waiting time.



12 Fig. 13. Comparison of waiting costs and waiting times with and without accurate ride-tide consideration.

13 Fig. 13(a) presents a comparison of the waiting costs between the algorithms that consider accurate ride-tide and
 14 those that do not. It is evident that algorithms that factor in the ride-tide information consistently outperform those
 15 that do not. The incorporation of precise tide conditions allows for more efficient scheduling, reducing unnecessary
 16 waiting times at port entrances, which directly translates to lower overall waiting costs. In contrast, the algorithms
 17 without ride-tide consideration exhibit higher waiting costs due to suboptimal scheduling that fails to align with the
 18 tide variations. This reinforces the importance of accurately accounting for ride-tide in maritime scheduling to achieve
 19 cost reductions. Fig. 13(b) shows the comparison of waiting times under both scenarios. As expected, the algorithms
 20 that integrate accurate ride-tide information also demonstrate reduced waiting times. The alignment of vessel arrivals
 21 with the optimal tide window minimizes the time vessels spend waiting to dock, leading to a smoother and more
 22 predictable port operation. On the other hand, when ride-tide factors are neglected, vessels experience extended wait-
 23 ing times, as their arrivals may not coincide with the most favorable tide conditions. This can lead to congestion and
 24 inefficiencies within the port, further exacerbating operational delays.

25 The results from both the waiting costs and waiting time comparisons clearly demonstrate the significant ad-
 26 vantages of incorporating accurate ride-tide into the algorithms. The reduction in waiting costs and waiting time
 27 reflects improved efficiency in port operations, highlighting the necessity of integrating environmental and opera-
 28 tional factors, such as tide conditions, into decision-making processes. These findings align with the broader objective
 29 of optimizing maritime scheduling to achieve both economic and environmental benefits, as minimizing waiting time
 30 and cost directly contributes to reducing fuel consumption and emissions during port operations.

6.3.8. Sensitivity analysis

(1) Analysis of the proportion of large-scale vessels

We selected benchmark instances comprising 20 inbound and 20 outbound vessels for our analysis. New instances were generated by varying the proportion of large-scale vessels, ranging from 0% to 50% in 5% increments. This approach was based on our research into the proportion of large-scale versus normal-draft vessels in some multi-functional ports, resulting in a total of 55 new instances (11 proportions of large vessels with 5 instances each). The detailed computational results are presented in Table 10, where “Gap” denotes the average difference in objective value between the improved B&P algorithm and the current real-world scheme (FCFS). The objective value curve, computational time curve, and average gap curve are depicted in Fig. 14.

Table 10

The detailed computational results with varying proportions of large-scale vessels.

The proportion of large-scale vessels	Average			FCFS	Gap (%)
	LB (million)	Obj (million)	Time (s)	Obj (million)	
0%	0.3560	0.3980	0.3020	0.3980	0.00%
5%	0.3890	0.4530	0.4140	0.5120	11.52%
10%	0.4350	0.5160	0.5560	0.6090	15.27%
15%	0.4610	0.5570	0.6980	0.6590	15.48%
20%	0.4992	0.5846	0.8740	0.7040	16.96%
25%	0.5550	0.6020	0.9980	0.7520	19.95%
30%	0.5970	0.6580	1.2050	0.9050	27.29%
35%	0.7540	0.8020	1.2730	1.1460	30.02%
40%	0.9020	0.9590	1.3120	1.6550	42.05%
45%	1.1080	1.1660	1.3590	2.4970	53.30%
50%	1.3870	1.4310	1.4020	4.3210	66.88%

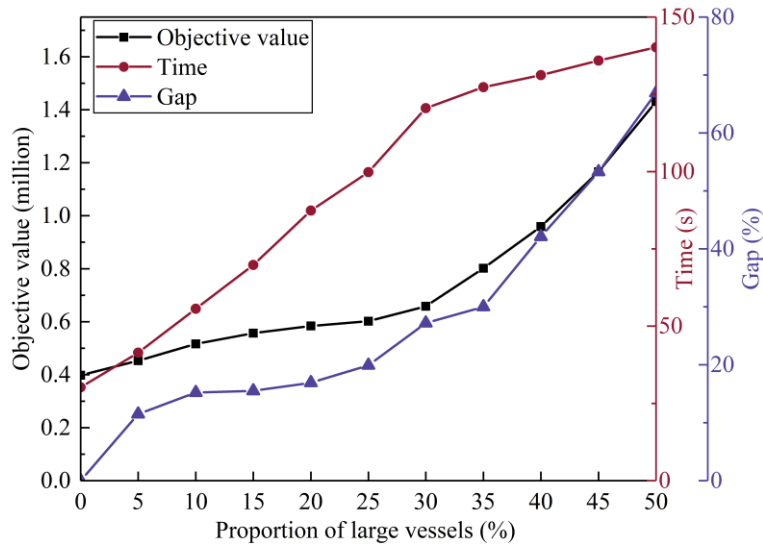


Fig. 14. Sensitivity analysis of the proportion of large-scale vessels.

The key insights from Table 10 and Fig. 14 can be summarized as follows: First, when the proportion of large-scale vessels is set to 0%, no vessel needs to ride-tide. Scheduled vessels are not constrained by ATTWs, rendering the situation a traditional vessel scheduling problem. In such cases, our proposed improved B&P algorithm resolves the problem in just half a minute, demonstrating its suitability for practical applications in ports without tidal channels. Second, as the proportion of large-scale vessels increases, so does the computational time, reflecting the growing complexity of the problem with more vessels requiring tidal riding. The objective value initially rises slowly and then

1 more rapidly, due to the increasing proportion of large vessels whose ATTW demands may exceed the channel's
 2 navigational capacity on a given day, forcing them to wait at anchor for the next day's ATTWs. Fig. 11 clearly shows
 3 that the performance gap widens with the increase in large-scale vessels, underscoring the superiority of our proposed
 4 B&P algorithm in handling more complex scenarios.

5 *(2) Analysis of the proportion of dangerous goods vessels*

6 As stated earlier, a significant contribution of this study is the consideration of the influence of dangerous goods
 7 vessels on the overall scheduling effectiveness. Additional computational experiments are carried out to examine the
 8 impact of dangerous goods vessels on the objective value and computational performance. We generate new instances
 9 using the group of instances comprising 20 inbound vessels and 20 outbound vessels. The proportion of dangerous
 10 goods vessels is varied from 0% to 100% in increments of 5%. Again, 5 instances for each group, totaling 105 in-
 11 stances are generated. The comprehensive computational results can be found in [Table 11](#) and [Fig. 15](#).

12 **Table 11**

13 The detailed computational results with varying proportions of dangerous goods vessels.

The proportion of dangerous goods vessels	Average			FCFS	Gap (%)
	LB (million)	Obj (million)	Time (s)	Obj (million)	
0%	0.2336	0.2740	0.2980	0.2740	0.00%
5%	0.2457	0.2910	0.3120	0.3220	9.63%
10%	0.2707	0.3260	0.3540	0.3840	15.10%
15%	0.2893	0.3520	0.3890	0.4250	17.18%
20%	0.3071	0.3770	0.4050	0.4650	18.92%
25%	0.3221	0.3980	0.4370	0.5010	20.56%
30%	0.3357	0.4170	0.4850	0.5540	24.73%
35%	0.3507	0.4380	0.5540	0.6010	27.12%
40%	0.3657	0.4590	0.6070	0.7080	35.17%
45%	0.3907	0.4940	0.6690	0.8530	42.09%
50%	0.4671	0.6010	0.7580	1.1040	45.56%
55%	0.5364	0.6980	0.8560	1.4020	50.21%
60%	0.6107	0.8020	0.9410	1.6210	50.52%
65%	0.6714	0.8870	1.0090	1.8060	50.89%
70%	0.7407	0.9840	1.1220	2.0050	50.92%
75%	0.3964	0.5020	0.5040	0.6040	16.89%
80%	0.3671	0.4610	0.4570	0.5410	14.79%
85%	0.3500	0.4370	0.3920	0.4970	12.07%
90%	0.3321	0.4120	0.3670	0.4620	10.82%
95%	0.2886	0.3510	0.3340	0.3910	10.23%
100%	0.2421	0.2860	0.2840	0.2860	0.00%

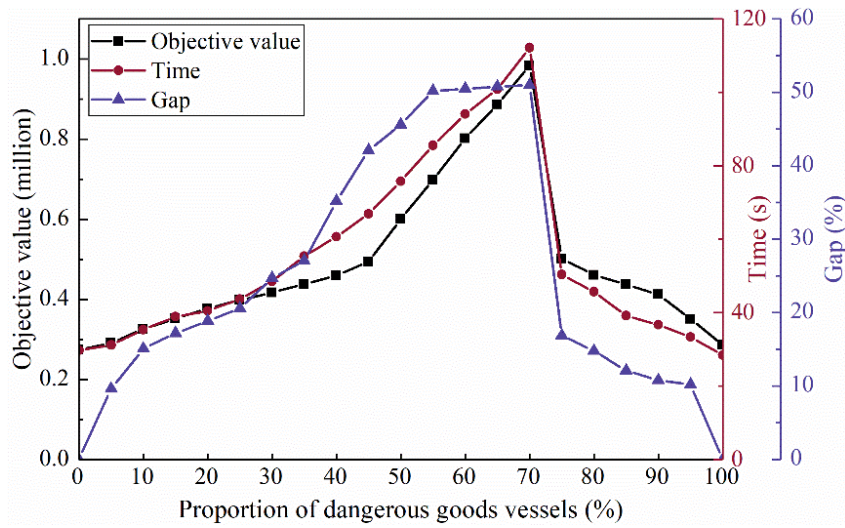


Fig. 15. Sensitivity analysis of the proportion of dangerous goods vessels.

In reality, scheduling vessels entering and leaving multi-functional ports with long channel links requires consideration of more complicated factors than in normal cases. The above analysis can assist port schedulers in making better trade-offs between economic benefits and time costs when planning scheduling. For example, an increase in the proportion of large-scale vessels within the scheme may decrease overall scheduling efficiency, while dominance of dangerous goods vessels in the scheme could reduce the objective value. As a result, port schedulers can make informed decisions regarding the percentage of large-scale vessels and dangerous goods vessels to include within a scheduling scheme to achieve optimal scheduling results. In addition, vessels can adjust their sailing speeds according to accurate ride-tide planning and vessel scheduling to reduce waiting time in ports, thereby alleviating port congestion and lowering the cost of berthing vessels. Simultaneously, shipping companies can adjust their fleet operations according to these plans, better organizing the use of vessels and crews, and improving the efficiency of resource utilization.

7. Conclusions

This paper has modeled and solved the joint accurate ride-tide planning and vessel scheduling problem for a long channel in a multi-function port. It first proposes the PSRT method to determine accurate ride-tide planning. To tackle the optimization challenge, a new model is constructed with a diagonal chunking structure based on the PSRT and then developed an improved B&P algorithm embedding three enhancement methods. The results of our extensive numerical experiments demonstrate that the improved B&P can yield near-optimal solutions within a much shorter computation time than a direct application of CPLEX and CG. In addition, in comparison to the real port scheduling schemes, the solutions obtained through the model and improved B&P algorithm significantly reduce the waiting costs of vessels. More importantly, the need for accurate ride-tide planning is not limited to multi-functional ports, other types of ports will also experience increased demand for accurate ride-tide planning as the size of vessels continues to grow. Based on our findings, some managerial implications can be recommended for port operators. It is economical to prioritize large-scale vessels ride-tide to enter or leave the port during the planned time. However, it is not recommended to concentrate exclusively on large vessels as this may impact the loading and unloading process at the port. Vessel scheduling operators can insert small-scale vessels between large-scale vessels. In addition, when scheduling different types of vessels simultaneously, it is recommended to prioritize faster vessels, such as container vessels, whenever possible, to avoid unnecessary waiting time in the channel and prevent overtaking situations.

This work could possibly be further extended and improved in the future. First, it assumes that the berths to which vessels are expected to call at before entering the port are idle. In reality, berth availability is influenced by the operational status of vessels in the port and the efficiency of loading and unloading equipment. Second, the investigated vessel scheduling issue represents a tactical-level planning challenge for port scheduling departments. Details

1 such as the specific loading and unloading workload for each cargo type and the actual arrival times of vessels remain
2 variable. Lastly, it is crucial to consider the integration of maritime and terrestrial scheduling challenges in port op-
3 erations to enhance overall efficiency. For instance, incorporating factors like the efficiency of port handling equip-
4 ment and vessel declaration procedures into the vessel scheduling process is helpful.

5 **Credit authorship contribution statement**

6 **Xinyu Zhang:** Conceptualization, Data curation, Funding acquisition, Methodology, Project administration,
7 Resources, Visualization, Writing-original draft. **Wenqiang Guo:** Conceptualization, Formal analysis, Investigation,
8 Methodology, Supervision, Software, Validation, Visualization, Writing-review & editing. **Zaili Yang:** Formal anal-
9 ysis, Investigation, Supervision, Validation, Writing-review & editing. **Jingyun Wang:** Supervision, Validation, Writ-
10 ing-review & editing. **Chengbo Wang:** Conceptualization, Formal analysis, Investigation.

11 **Declaration of interest statement**

12 The authors declare that they have no known competing financial interests or personal relationships that could
13 have appeared to influence the work reported in this paper.

14 **Data availability**

15 Data will be made available on request.

16 **Acknowledgments**

17 This work was supported by the National Natural Science Foundation of China [grant number 52371359].

18 **References**

- 19 Chen, X. (2023) Vessel scheduling optimization under the condition of compound waterway (Master's thesis). Dalian
20 Maritime University, Dalian.
- 21 Clarksons. Shipping Intelligence Network. Retrieved from <https://www.clarksons.net.cn>. Accessed March 30, 2023.
- 22 Corry, P., & Bierwirth, C. (2019). The berth allocation problem with channel restrictions. *Transportation Science*,
23 53(3), 708-727. DOI: <https://doi.org/10.1287/trsc.2018.0865>.
- 24 Dadashi, A., Dulebenets, M. A., Golias, M. M., & Sheikholeslami, A. (2017). A novel continuous berth scheduling
25 model at multiple marine container terminals with tidal considerations. *Maritime Business Review*, 2(2), 142-
26 157. DOI: <https://doi.org/10.1108/MABR-02-2017-0010>.
- 27 De, A., Choudhary, A., & Tiwari, M. K. (2017). Multiobjective approach for sustainable ship routing and scheduling
28 with draft restrictions. *IEEE Transactions on Engineering Management*, 66(1), 35-51.
29 DOI: <https://doi.org/10.1109/TEM.2017.2766443>.
- 30 Du, Y., Chen, Q., Lam, J. S. L., Xu, Y., & Cao, J. X. (2015). Modeling the impacts of tides and the virtual arrival
31 policy in berth allocation. *Transportation Science*, 49(4), 939-956.
32 DOI: <https://doi.org/10.1287/trsc.2014.0568>.
- 33 Dulebenets, M. A., Pasha, J., Abioye, O. F., & Kavooosi, M. (2021). Vessel scheduling in liner shipping: A critical
34 literature review and future research needs. *Flexible Services and Manufacturing Journal*, 33, 43-106.
35 DOI: <https://doi.org/10.1007/s10696-019-09367-2>.
- 36 Gao, Y., & Sun, Z. (2023). Tramp ship routing and speed optimization with tidal berth time windows. *Transportation*
37 *Research Part E: Logistics and Transportation Review*, 178, 103268.
38 DOI: <https://doi.org/10.1016/j.tre.2023.103268>
- 39 Halvorsen-Weare, E. E., & Fagerholt, K. (2013). Routing and scheduling in a liquefied natural gas shipping problem
40 with inventory and berth constraints. *Annals of Operations Research*, 203, 167-186.
41 DOI: <https://doi.org/10.1007/s10479-010-0794-y>.

- 1 Halvorsen-Weare, E. E., Fagerholt, K., & Rönnqvist, M. (2013). Vessel routing and scheduling under uncertainty in
2 the liquefied natural gas business. *Computers & Industrial Engineering*, 64(1), 290-301.
3 DOI: <https://doi.org/10.1016/j.cie.2012.10.011>.
- 4 Hansen, P., & Mladenović, N. (2001). Variable neighborhood search: Principles and applications. *European journal*
5 *of operational research*, 130(3), 449-467. DOI: [https://doi.org/10.1016/S0377-2217\(00\)00100-4](https://doi.org/10.1016/S0377-2217(00)00100-4).
- 6 Hsu, K. Y., Kou, T. C., & Wu, Z. L. (2008). Optimum scheduling model for ship in/outbound harbor in one-way
7 traffic fairway. *Journal of Dalian Maritime University*, 4(24), 038.
8 DOI:10.16411/j.cnki.issn1006-7736.2008.04.011.
- 9 Jia, S., Li, C. L., & Xu, Z. (2019). Managing navigation channel traffic and anchorage area utilization of a container
10 port. *Transportation Science*, 53(3), 728-745. DOI: <https://doi.org/10.1287/trsc.2018.0879>.
- 11 Jiang, X., Zhong, M., Shi, J., & Li, W. (2024). Optimization of integrated scheduling of restricted channels, berths,
12 and yards in bulk cargo ports considering carbon emissions. *Expert Systems with Applications*, 255, 124604.
13 DOI: <https://doi.org/10.1016/j.eswa.2024.124604>.
- 14 Kellerer, H., Pferschy, U., Pisinger, D., Kellerer, H., Pferschy, U., & Pisinger, D. (2004). Introduction to NP-Com-
15 pleteness of knapsack problems. *Knapsack problems*, 483-493. DOI: https://doi.org/10.1007/978-3-540-24777-7_16
- 16
- 17 Ksciuk, J., Kuhlemann, S., Tierney, K., & Koberstein, A. (2023). Uncertainty in maritime ship routing and scheduling:
18 A Literature review. *European Journal of Operational Research*, 308(2), 499-524.
19 DOI: <https://doi.org/10.1016/j.ejor.2022.08.006>.
- 20 La Scalia, G., Mancini, S., Adelfio, L., & Giallanza, A. (2023). Development of a Vessel Scheduling Optimization
21 Model to improve Maritime Transport sustainability. *Sustainable Futures*, 6, 100123.
22 DOI: <https://doi.org/10.1016/j.sftr.2023.100123>.
- 23 Lalla-Ruiz, E., Shi, X., & Voß, S. (2018). The waterway ship scheduling problem. *Transportation Research Part D:*
24 *Transport and Environment*, 60, 191-209. DOI: <https://doi.org/10.1016/j.trd.2016.09.013>.
- 25 Le Carrer, N., Ferson, S., & Green, P. L. (2020). Optimising cargo loading and ship scheduling in tidal areas. *Euro-*
26 *pean Journal of Operational Research*, 280(3), 1082-1094. DOI: <https://doi.org/10.1016/j.ejor.2019.08.002>.
- 27 Li, R., Zhang, X., Jiang, L., Yang, Z., & Guo, W. (2022). An adaptive heuristic algorithm based on reinforcement
28 learning for ship scheduling optimization problem. *Ocean & Coastal Management*, 230, 106375.
29 DOI: <https://doi.org/10.1016/j.ocecoaman.2022.106375>.
- 30 Liu, B., Li, Z. C., Wang, Y., & Sheng, D. (2021). Short-term berth planning and ship scheduling for a busy seaport
31 with channel restrictions. *Transportation Research Part E: Logistics and Transportation Review*, 154, 102467.
32 DOI: <https://doi.org/10.1016/j.tre.2021.102467>.
- 33 Liu, C., Wen, J., & Liu, N. (2024, February). Ship scheduling optimization in restricted two-way channel ports. In
34 *International Conference on Smart Transportation and City Engineering (STCE 2023)* (Vol. 13018, pp. 1515-
35 1521). SPIE. DOI: <https://doi.org/10.1117/12.3024034>
- 36 Liu, D., Shi, G., & Hirayama, K. (2021). Vessel scheduling optimization model based on variable speed in a seaport
37 with one-way navigation channel. *Sensors*, 21(16), 5478. DOI: <https://doi.org/10.3390/s21165478>.
- 38 MOT, Port infrastructure maintenance regulations, Retrieved from <https://xxgk.mot.gov.cn>. Accessed March 19,
39 2023
- 40 Meng, Q., Wang, S., Andersson, H., & Thun, K. (2014). Containership routing and scheduling in liner shipping:
41 overview and future research directions. *Transportation Science*, 48(2), 265-280.
42 DOI: <https://doi.org/10.1287/trsc.2013.0461>.
- 43 Noshokaty, S. E. (2023). Shipping optimisation systems for liner: en-route bunkering, port late arrival, and tide re-
44 stricted sailing. *International Journal of Shipping and Transport Logistics*, 16(1-2), 154-169.
45 DOI: <https://doi.org/10.1504/IJSTL.2023.128573>
- 46 Qiang, L., Bing-Dong, Y., & Bi-Guang, H. (2018). Calculation and measurement of tide height for the navigation of
47 ship at high tide using artificial neural network. *Polish Maritime Research*, 25(s3), 99-110.

1 DOI: <https://doi.org/10.2478/pomr-2018-0118>.

2 Qiao, G.Q., Wang, C.X., & Zhou, H.C. (2020). Navigable window period and waiting time at tide riding water level.
3 *Port and Waterway Engineering*, 11 (575), 40-47+62.
4 DOI:10.16233/j.cnki.issn1002-4972.20201102.032.

5 Shao, X., & Xin, Y. (2019). A scheduling algorithm based on the singular value decomposition heuristic method in
6 a distributed manufacturing system. *Expert Systems*, 36(4), e12433. DOI: <https://doi.org/10.1111/exsy.12433>.

7 Shen, H., Shu, S., Qin, H., & Wu, Q. (2020). An exact algorithm for the multi-period inspector scheduling problem.
8 *Computers & Industrial Engineering*, 145, 106515. DOI: <https://doi.org/10.1016/j.cie.2020.106515>.

9 Tang, S., Xu, S., Gao, J., Ma, M., & Liao, P. (2022). Effect of service priority on the integrated continuous berth
10 allocation and quay crane assignment problem after port congestion. *Journal of Marine Science and Engineering*,
11 10(9), 1259. DOI: <https://doi.org/10.3390/jmse10091259>.

12 Wang, S., & Meng, Q. (2017). Container liner fleet deployment: A systematic overview. *Transportation Research*
13 *Part C: Emerging Technologies*, 77, 389-404. DOI: <https://doi.org/10.1016/j.trc.2017.02.010>.

14 Wu, W. M. (2020). The optimal speed in container shipping: Theory and empirical evidence. *Transportation Re-*
15 *search Part E: Logistics and Transportation Review*, 136, 101903.
16 DOI: <https://doi.org/10.1016/j.tre.2020.101903>.

17 Xe, F.R. (2017). Branch and price algorithm for the integrated berth allocation and quay crane assignment (Master's
18 Thesis) Tsinghua University, Beijing.

19 Yan, R., Wang, S., & Du, Y. (2020). Development of a two-stage ship fuel consumption prediction and reduction
20 model for a dry bulk ship. *Transportation Research Part E: Logistics and Transportation Review*, 138, 101930.
21 DOI: <https://doi.org/10.1016/j.tre.2020.101930>.

22 Yang, X., Gu, W., & Wang, S. (2023). Optimal scheduling of vessels passing a waterway bottleneck. *Ocean &*
23 *Coastal Management*, 244, 106809. DOI: <https://doi.org/10.1016/j.ocecoaman.2023.106809>.

24 Zhang, B., Zheng, Z., & Wang, D. (2020). A model and algorithm for vessel scheduling through a two-way tidal
25 channel. *Maritime Policy & Management*, 47(2), 188-202.
26 DOI: <https://doi.org/10.1080/03088839.2019.1676477>

27 Zhang, J., Santos, T. A., Guedes Soares, C., & Yan, X. (2017). Sequential ship traffic scheduling model for restricted
28 two-way waterway transportation. *Proceedings of the Institution of Mechanical Engineers, Part M: Journal of*
29 *Engineering for the Maritime Environment*, 231(1), 86-97.
30 DOI: <https://doi.org/10.1177/1475090215621580>.

31 Zhang, X., Li, R., Chen, X., Li, J., & Wang, C. (2019). Multi-object-based vessel traffic scheduling optimisation in
32 a compound waterway of a large harbour. *The Journal of Navigation*, 72(3), 609-627.
33 DOI: <https://doi.org/10.1017/S0373463318000863>.

34 Zhang, X.Y., Guo, W.Q., Wang, J.Y., & Yang, B.D. (2022) Research on the refined segmental tide riding of large
35 vessels based on multi-source maritime data. *Journal of Geo-Information Science*, 24 (9) 1688–1700.
36 DOI: <https://doi.org/10.12082/dqxxkx.2022.210710>.

37 Zhang, Y., Liu, S., Zheng, Q., Tian, H., & Guo, W. (2024). Ship scheduling problem in an anchorage-to-quay channel
38 with water discharge restrictions. *Ocean Engineering*, 309, 118432.
39 DOI: <https://doi.org/10.1016/j.oceaneng.2024.118432>.

40 Zhao, K., Jin, J. G., Zhang, D., Ji, S., & Lee, D. H. (2023). A variable neighborhood search heuristic for real-time
41 barge scheduling in a river-to-sea channel with tidal restrictions. *Transportation Research Part E: Logistics and*
42 *Transportation Review*, 179, 103280. DOI: <https://doi.org/10.1016/j.tre.2023.103280>

43 Zhao, K., Zhang, D., Jin, J. G., Dong, G., & Lee, D. H. (2024). Vessel voyage schedule planning for maritime ore
44 transportation. *Ocean Engineering*, 291, 116503. DOI: <https://doi.org/10.1016/j.oceaneng.2023.116503>.

45 Zhen, L., Liang, Z., Zhuge, D., Lee, L. H., & Chew, E. P. (2017). Daily berth planning in a tidal port with channel
46 flow control. *Transportation Research Part B: Methodological*, 106, 193-217.
47 DOI: <https://doi.org/10.1016/j.trb.2017.10.008>.

- 1 Zhong, H., Zhang, Y., & Gu, Y. (2022). A Bi-objective green tugboat scheduling problem with the tidal port time
2 windows. *Transportation Research Part D: Transport and Environment*, 110, 103409.
3 DOI: <https://doi.org/10.1016/j.trd.2022.103409>
- 4 Özlem, Ş., Or, İ., & Altan, Y. C. (2021). Scheduling and simulation of maritime traffic in congested waterways: An
5 application to the Strait of Istanbul. *The Journal of Navigation*, 74(3), 656-672.
6 DOI: <https://doi.org/10.1017/S0373463320000715>.

1 **Appendix A**

2 Tables A1-A3 report the detailed computational results of [Table 6](#) for the low traffic flow, medium traffic flow, and heavy
3 traffic flow, respectively.

4 **Table A 1**

5 Details of the computational results reported in Table 6 (low traffic flow).

Group	Instance	B&P			CG			CPLEX			IGA	
		LB (million)	Obj (million)	Time (s)	LB (million)	Obj (million)	Time (s)	LB (million)	Obj (million)	Time (s)	Obj (million)	Time (s)
L_5_5	1	0.122	0.124	5.36	0.122	0.124	5.78	0.124	0.124	16.49	0.149	4.52
	2	0.110	0.110	5.57	0.110	0.110	6.30	0.110	0.110	16.70	0.127	4.62
	3	0.120	0.121	5.04	0.118	0.123	6.20	0.121	0.121	17.22	0.141	4.41
	4	0.113	0.118	5.15	0.113	0.118	6.41	0.118	0.118	16.59	0.145	4.41
	5	0.110	0.114	4.73	0.110	0.111	5.04	0.114	0.114	15.12	0.130	4.20
AVE	--	0.115	0.117	5.17	0.115	0.117	5.94	0.117	0.117	16.42	0.138	4.43
L_5_9	1	0.124	0.126	6.51	0.124	0.126	7.56	0.126	0.126	16.91	0.156	4.94
	2	0.129	0.130	6.30	0.128	0.129	7.46	0.130	0.130	17.12	0.175	4.83
	3	0.126	0.127	6.09	0.126	0.127	8.30	0.127	0.127	16.49	0.152	4.83
	4	0.114	0.120	5.36	0.114	0.120	6.51	0.120	0.120	16.28	0.145	4.52
	5	0.125	0.125	5.15	0.125	0.125	5.99	0.125	0.125	17.22	0.154	4.41
AVE	--	0.124	0.126	5.88	0.123	0.125	7.16	0.126	0.126	16.80	0.157	4.70
L_5_12	1	0.121	0.124	6.51	0.121	0.124	6.83	0.124	0.124	17.64	0.130	4.94
	2	0.123	0.123	7.56	0.123	0.124	7.77	0.123	0.123	17.96	0.125	5.36
	3	0.120	0.122	6.20	0.120	0.122	6.72	0.122	0.122	18.27	0.123	4.83
	4	0.122	0.123	5.36	0.122	0.123	6.20	0.123	0.123	18.17	0.162	4.52
	5	0.121	0.126	7.46	0.121	0.126	8.82	0.126	0.126	18.90	0.137	5.36
AVE	--	0.121	0.123	6.62	0.121	0.124	7.27	0.123	0.123	18.19	0.135	5.00
L_9_5	1	0.113	0.119	7.77	0.113	0.121	9.14	0.119	0.119	16.17	0.125	5.46
	2	0.109	0.116	8.93	0.109	0.117	10.29	0.116	0.116	16.38	0.130	5.88
	3	0.124	0.130	6.72	0.124	0.134	8.19	0.130	0.130	16.59	0.149	5.04
	4	0.126	0.128	7.14	0.126	0.130	9.14	0.128	0.128	15.96	0.152	5.25
	5	0.127	0.127	7.46	0.127	0.129	9.87	0.127	0.127	16.49	0.154	5.36
AVE	--	0.120	0.124	7.60	0.120	0.126	9.32	0.124	0.124	16.32	0.142	5.40
L_9_9	1	0.126	0.126	7.77	0.126	0.130	9.56	0.126	0.126	16.80	0.162	5.46
	2	0.125	0.125	8.09	0.125	0.125	9.14	0.125	0.125	17.64	0.166	5.67
	3	0.130	0.132	7.98	0.129	0.133	9.24	0.132	0.132	17.75	0.175	5.57
	4	0.119	0.121	6.83	0.119	0.126	7.77	0.121	0.121	17.54	0.141	5.04
	5	0.129	0.129	5.15	0.129	0.133	6.72	0.129	0.129	17.01	0.152	4.41
AVE	--	0.126	0.127	7.16	0.126	0.130	8.48	0.127	0.127	17.35	0.159	5.23
L_9_12	1	0.142	0.144	8.30	0.142	0.146	9.14	0.144	0.144	17.85	0.163	5.67
	2	0.143	0.148	8.61	0.143	0.148	10.19	0.148	0.148	19.01	0.176	5.78
	3	0.141	0.145	6.83	0.141	0.149	9.24	0.145	0.145	19.11	0.176	5.04
	4	0.135	0.141	7.77	0.135	0.141	8.30	0.141	0.141	19.53	0.165	5.46
	5	0.126	0.126	8.82	0.126	0.129	9.56	0.126	0.126	18.69	0.133	5.88
AVE	--	0.137	0.141	8.06	0.137	0.143	9.28	0.141	0.141	18.84	0.163	5.57
L_12_5	1	0.145	0.147	9.35	0.145	0.150	11.03	0.147	0.147	15.75	0.187	6.09
	2	0.152	0.153	8.19	0.152	0.154	10.19	0.153	0.153	19.85	0.186	5.67
	3	0.187	0.189	5.36	0.187	0.194	7.46	0.189	0.189	20.06	0.198	4.52
	4	0.153	0.153	7.46	0.153	0.154	9.35	0.153	0.153	20.16	0.172	5.36
	5	0.152	0.152	6.30	0.152	0.156	7.04	0.152	0.152	21.53	0.184	4.83
AVE	--	0.158	0.159	7.33	0.158	0.162	9.01	0.159	0.159	19.47	0.185	5.29
L_12_9	1	0.160	0.161	9.35	0.160	0.165	10.40	0.161	0.161	20.27	0.204	6.09
	2	0.164	0.165	9.56	0.164	0.168	10.92	0.165	0.165	20.37	0.172	6.20
	3	0.155	0.155	9.87	0.155	0.155	11.45	0.155	0.155	21.42	0.179	6.30
	4	0.153	0.156	8.93	0.153	0.160	10.71	0.156	0.156	22.58	0.196	5.88
	5	0.158	0.160	9.77	0.158	0.162	11.66	0.160	0.160	22.47	0.175	6.30
AVE	--	0.158	0.159	9.49	0.158	0.162	11.03	0.159	0.159	21.42	0.185	6.15
L_12_12	1	0.165	0.167	10.29	0.165	0.169	11.97	0.167	0.167	22.89	0.211	6.51
	2	0.162	0.162	10.50	0.162	0.165	12.50	0.162	0.162	21.95	0.172	6.62
	3	0.169	0.169	11.24	0.169	0.171	12.71	0.169	0.169	22.47	0.204	6.83
	4	0.176	0.181	10.92	0.176	0.185	12.29	0.181	0.181	22.37	0.191	6.72
	5	0.169	0.173	9.98	0.169	0.174	11.24	0.173	0.173	22.79	0.188	6.30
AVE	--	0.168	0.170	10.58	0.168	0.173	12.14	0.170	0.170	22.49	0.193	6.59

1 **Table A 2**

2 Details of the computational results reported in Table 6 (medium traffic flow).

Group	In-stance	B&P			CG			CPLEX			IGA	
		LB (million)	Obj (million)	Time (s)	LB (million)	Obj (million)	Time (s)	LB (million)	Obj (million)	Time (s)	Obj (million)	Time (s)
M_13_13	1	0.320	0.340	19.30	0.320	0.420	34.10	0.340	0.340	111.72	0.377	16.37
	2	0.290	0.302	19.91	0.290	0.373	35.22	0.302	0.302	114.20	0.336	16.86
	3	0.309	0.331	19.06	0.309	0.409	33.73	0.331	0.331	110.73	0.367	16.12
	4	0.298	0.322	18.94	0.298	0.399	33.48	0.322	0.322	110.24	0.358	16.00
	5	0.290	0.314	17.12	0.290	0.388	30.38	0.314	0.314	102.67	0.348	14.51
AVE	--	0.301	0.322	18.87	0.301	0.398	33.38	0.322	0.322	109.91	0.357	15.97
M_13_15	1	0.326	0.346	25.98	0.326	0.427	45.63	0.346	0.346	139.38	0.383	22.07
	2	0.337	0.357	25.13	0.337	0.442	44.14	0.357	0.357	135.90	0.396	21.33
	3	0.331	0.348	25.49	0.331	0.431	44.89	0.348	0.348	137.52	0.386	21.70
	4	0.301	0.328	21.25	0.301	0.406	37.57	0.328	0.328	119.91	0.364	17.98
	5	0.328	0.343	21.12	0.328	0.424	37.32	0.343	0.343	119.29	0.380	17.86
AVE	--	0.325	0.344	23.79	0.325	0.426	41.91	0.344	0.344	130.40	0.382	20.19
M_13_17	1	0.317	0.340	25.74	0.317	0.420	45.38	0.340	0.340	138.51	0.377	21.82
	2	0.323	0.337	24.40	0.323	0.417	43.03	0.337	0.337	132.93	0.374	20.71
	3	0.315	0.334	24.52	0.315	0.413	43.52	0.334	0.334	134.04	0.370	20.96
	4	0.320	0.337	21.73	0.320	0.417	38.32	0.337	0.337	121.89	0.374	18.48
	5	0.317	0.346	29.74	0.317	0.427	52.33	0.346	0.346	155.37	0.383	25.30
AVE	--	0.318	0.339	25.23	0.319	0.419	44.52	0.339	0.339	136.55	0.375	21.45
M_15_13	1	0.298	0.325	31.08	0.298	0.402	54.56	0.325	0.325	160.70	0.361	26.41
	2	0.287	0.317	35.69	0.287	0.391	62.74	0.317	0.317	180.30	0.352	30.50
	3	0.326	0.357	27.56	0.326	0.442	48.48	0.357	0.357	146.07	0.396	23.44
	4	0.331	0.351	28.53	0.331	0.435	50.10	0.351	0.351	150.04	0.389	24.30
	5	0.334	0.348	29.74	0.334	0.431	52.33	0.348	0.348	155.37	0.386	25.30
AVE	--	0.315	0.340	30.52	0.315	0.420	53.64	0.340	0.340	158.50	0.377	25.99
M_15_15	1	0.331	0.346	31.08	0.331	0.427	54.56	0.346	0.346	160.70	0.383	26.41
	2	0.328	0.343	32.05	0.328	0.424	56.30	0.343	0.343	164.80	0.380	27.28
	3	0.342	0.363	31.69	0.342	0.449	56.05	0.363	0.363	164.30	0.402	27.16
	4	0.312	0.331	27.19	0.312	0.409	47.86	0.331	0.331	144.71	0.367	23.19
	5	0.339	0.354	20.40	0.339	0.438	36.08	0.354	0.354	116.31	0.392	17.36
AVE	--	0.331	0.347	28.48	0.331	0.430	50.17	0.347	0.347	150.16	0.385	24.28
M_15_17	1	0.373	0.395	33.14	0.373	0.489	58.28	0.395	0.395	169.63	0.436	28.27
	2	0.375	0.406	34.48	0.375	0.503	60.51	0.406	0.406	174.96	0.449	29.39
	3	0.370	0.397	27.19	0.370	0.492	47.86	0.397	0.397	144.71	0.440	23.19
	4	0.356	0.386	32.05	0.356	0.478	56.30	0.386	0.386	164.80	0.427	27.28
	5	0.331	0.346	35.33	0.331	0.427	62.00	0.346	0.346	178.44	0.383	30.13
AVE	--	0.361	0.386	32.44	0.361	0.478	56.99	0.386	0.386	166.51	0.427	27.65
M_17_13	1	0.381	0.403	37.39	0.381	0.499	65.72	0.403	0.403	187.36	0.446	31.87
	2	0.400	0.421	32.78	0.400	0.521	57.54	0.421	0.421	167.77	0.465	27.90
	3	0.491	0.518	23.55	0.491	0.643	41.54	0.518	0.518	129.46	0.572	19.96
	4	0.403	0.421	29.74	0.403	0.521	52.33	0.421	0.421	155.37	0.465	25.30
	5	0.400	0.418	29.74	0.400	0.517	52.33	0.418	0.418	155.25	0.462	25.30
AVE	--	0.415	0.436	30.64	0.415	0.540	53.89	0.436	0.436	159.04	0.482	26.06
M_17_15	1	0.420	0.441	37.39	0.420	0.546	65.72	0.441	0.441	187.36	0.487	31.87
	2	0.431	0.452	38.36	0.431	0.560	67.08	0.452	0.452	190.96	0.499	32.61
	3	0.408	0.426	38.24	0.408	0.528	67.08	0.426	0.426	190.59	0.471	32.61
	4	0.403	0.429	35.69	0.403	0.532	62.74	0.429	0.429	180.30	0.474	30.50
	5	0.414	0.438	39.21	0.414	0.542	68.57	0.438	0.438	194.43	0.484	33.36
AVE	--	0.415	0.437	37.78	0.415	0.542	66.24	0.437	0.437	188.73	0.483	32.19
M_17_17	1	0.433	0.458	41.28	0.433	0.567	72.29	0.458	0.458	203.36	0.506	35.22
	2	0.425	0.444	41.52	0.425	0.550	72.54	0.444	0.444	203.86	0.490	35.34
	3	0.444	0.464	40.30	0.444	0.575	70.68	0.464	0.464	199.27	0.512	34.35
	4	0.464	0.495	43.83	0.464	0.614	76.76	0.495	0.495	214.02	0.546	37.45
	5	0.444	0.475	40.91	0.444	0.589	71.67	0.475	0.475	201.75	0.524	34.84
AVE	--	0.442	0.467	41.57	0.442	0.579	72.79	0.467	0.467	204.45	0.516	35.44

3

1 **Table A 3**

2 Details of the computational results reported in Table 6 (heavy traffic flow).

Group	Instance	B&P			CG			CPLEX			IGA	
		LB (million)	Obj (million)	Time (s)	LB (million)	Obj (million)	Time (s)	LB (million)	Obj (million)	Time (s)	LB (million)	Time (s)
H_18_18	1	0.627	0.735	78.00	0.627	0.820	257.53	0.635	0.668	865.06	0.920	67.97
	2	0.568	0.670	80.34	0.568	0.753	264.55	0.576	0.607	890.26	0.839	69.63
	3	0.614	0.720	77.09	0.614	0.804	254.80	0.622	0.654	854.98	0.901	67.33
	4	0.600	0.705	76.57	0.600	0.789	253.37	0.608	0.640	849.94	0.883	67.07
	5	0.529	0.626	69.68	0.586	0.708	232.31	0.626	0.626	774.34	0.785	62.21
AVE	--	0.588	0.691	76.34	0.599	0.775	252.51	0.613	0.639	846.92	0.866	66.84
H_18_20	1	0.636	0.745	103.61	0.636	0.830	334.36	0.644	0.677	1140.86	0.932	85.63
	2	0.654	0.765	100.36	0.654	0.851	324.48	0.662	0.696	1105.44	0.957	83.33
	3	0.641	0.750	101.92	0.641	0.835	329.16	0.649	0.682	1122.10	0.938	84.48
	4	0.609	0.715	85.54	0.609	0.799	280.15	0.617	0.649	946.26	0.895	73.22
	5	0.632	0.668	85.02	0.632	0.825	278.59	0.668	0.672	940.66	0.926	72.83
AVE	--	0.634	0.729	95.29	0.634	0.828	309.35	0.648	0.675	1051.06	0.930	79.90
H_18_24	1	0.627	0.735	102.83	0.627	0.820	332.02	0.635	0.668	1132.18	0.920	85.12
	2	0.623	0.730	97.76	0.623	0.815	316.55	0.631	0.663	1076.74	0.914	81.54
	3	0.618	0.725	98.67	0.618	0.810	319.54	0.626	0.658	1087.80	0.908	82.30
	4	0.623	0.730	87.36	0.623	0.815	285.61	0.631	0.663	965.86	0.914	74.50
	5	0.636	0.745	118.43	0.636	0.830	378.69	0.644	0.677	1300.04	0.932	95.87
AVE	--	0.625	0.733	101.01	0.625	0.818	326.48	0.633	0.666	1112.52	0.917	83.87
H_20_18	1	0.605	0.710	123.37	0.605	0.794	393.51	0.613	0.644	1353.10	0.889	99.20
	2	0.591	0.695	141.44	0.591	0.779	447.72	0.599	0.630	1547.70	0.870	111.74
	3	0.654	0.765	109.85	0.654	0.851	353.08	0.662	0.696	1207.78	0.957	89.98
	4	0.645	0.755	113.49	0.645	0.841	364.00	0.653	0.686	1246.98	0.945	92.42
	5	0.641	0.750	118.43	0.641	0.835	378.69	0.649	0.682	1300.04	0.938	95.87
AVE	--	0.627	0.735	121.32	0.627	0.820	387.40	0.635	0.668	1331.12	0.920	97.84
H_20_20	1	0.636	0.745	123.37	0.636	0.830	393.51	0.644	0.677	1353.10	0.932	99.20
	2	0.632	0.740	127.14	0.632	0.825	404.95	0.640	0.672	1394.26	0.926	101.89
	3	0.663	0.775	126.62	0.663	0.861	403.39	0.671	0.705	1388.52	0.969	101.50
	4	0.614	0.720	108.55	0.614	0.804	349.18	0.622	0.654	1193.92	0.901	89.09
	5	0.650	0.760	82.29	0.650	0.846	270.27	0.658	0.691	910.84	0.951	70.91
AVE	--	0.639	0.748	113.59	0.639	0.833	364.26	0.647	0.680	1248.13	0.936	92.52
H_20_24	1	0.713	0.831	131.56	0.713	0.918	418.21	0.721	0.756	1441.58	1.037	104.96
	2	0.731	0.851	136.50	0.731	0.938	432.90	0.776	0.775	1494.64	1.062	108.29
	3	0.718	0.836	108.55	0.718	0.923	349.18	0.726	0.761	1193.92	1.044	89.09
	4	0.700	0.816	127.14	0.700	0.902	404.95	0.708	0.743	1394.26	1.019	101.89
	5	0.636	0.745	139.75	0.636	0.830	442.78	0.644	0.677	1530.06	0.932	110.59
AVE	--	0.700	0.816	128.70	0.700	0.902	409.60	0.715	0.742	1410.89	1.019	102.96
H_24_18	1	0.727	0.846	148.07	0.727	0.933	467.48	0.735	0.771	1618.54	1.056	116.22
	2	0.754	0.876	130.00	0.754	0.964	413.27	0.762	0.799	1423.94	1.093	103.81
	3	0.908	1.047	94.38	0.908	1.140	306.67	0.916	0.958	1041.46	1.304	79.23
	4	0.754	0.876	118.30	0.754	0.964	378.69	0.762	0.799	1300.04	1.093	95.87
	5	0.749	0.871	118.30	0.749	0.959	378.30	0.758	0.794	1298.50	1.087	95.74
AVE	--	0.778	0.903	121.81	0.778	0.992	388.88	0.787	0.824	1336.50	1.127	98.18
H_24_20	1	0.786	0.911	148.07	0.786	1.000	467.48	0.794	0.831	1618.54	1.137	116.22
	2	0.804	0.931	151.32	0.804	1.021	477.36	0.812	0.850	1653.96	1.161	118.53
	3	0.763	0.886	151.06	0.763	0.975	476.58	0.771	0.808	1651.30	1.106	118.27
	4	0.767	0.891	141.44	0.767	0.980	447.72	0.776	0.813	1547.70	1.112	111.74
	5	0.781	0.906	154.57	0.781	0.995	487.11	0.827	0.827	1689.24	1.130	120.70
AVE	--	0.780	0.905	149.29	0.780	0.994	471.25	0.796	0.826	1632.15	1.129	117.09
H_24_24	1	0.813	0.941	162.76	0.813	1.031	511.81	0.821	0.859	1777.72	1.174	126.46
	2	0.790	0.916	163.28	0.790	1.006	513.11	0.798	0.836	1782.34	1.143	126.72
	3	0.822	0.951	158.99	0.822	1.042	500.50	0.830	0.869	1736.98	1.186	123.78
	4	0.871	1.007	172.64	0.871	1.098	541.32	0.880	0.920	1883.84	1.254	133.25
	5	0.840	0.972	161.33	0.840	1.062	507.52	0.848	0.887	1762.18	1.211	125.44
AVE	--	0.827	0.957	163.80	0.827	1.048	514.85	0.836	0.874	1788.61	1.193	127.13

3

Appendix B

Tables B1-B3 report the detailed computational results of Fig. 8 for the low traffic flow, medium traffic flow, and heavy traffic flow, respectively.

Table B 1

Details of the computational results reported in Fig. 8 (low traffic flow).

Group	Instance	B&P		B&P_No_ISGS		B&P_No_OPVB		B&P_No_HLSA	
		Obj (million)	Time (s)	Obj (million)	Time (s)	Obj (million)	Time (s)	Obj (million)	Time (s)
L_5_5	1	0.124	5.36	0.124	15.18	0.124	65.89	0.124	181.06
	2	0.110	5.57	0.110	15.84	0.110	68.20	0.110	188.10
	3	0.121	5.04	0.121	14.08	0.121	62.37	0.121	170.61
	4	0.118	5.15	0.118	14.85	0.118	64.68	0.118	177.65
	5	0.114	4.73	0.114	12.98	0.114	58.74	0.114	160.16
AVE	--	0.117	5.17	0.117	14.59	0.117	63.98	0.117	175.52
L_5_9	1	0.126	6.51	0.126	18.92	0.126	78.87	0.126	219.45
	2	0.130	6.30	0.130	18.26	0.130	76.56	0.130	212.41
	3	0.127	6.09	0.127	17.49	0.127	74.14	0.127	205.48
	4	0.120	5.36	0.120	15.18	0.120	65.89	0.120	181.06
	5	0.125	5.15	0.125	14.41	0.125	63.47	0.125	174.13
AVE	--	0.126	5.88	0.126	16.85	0.126	71.79	0.126	198.51
L_5_12	1	0.124	6.51	0.124	18.92	0.124	78.87	0.124	219.45
	2	0.123	7.56	0.123	22.33	0.123	90.64	0.123	254.21
	3	0.122	6.20	0.122	17.93	0.122	75.35	0.122	209.00
	4	0.123	5.36	0.123	15.18	0.123	65.89	0.123	181.06
	5	0.126	7.46	0.126	22.00	0.126	89.54	0.126	250.80
AVE	--	0.123	6.62	0.123	19.27	0.123	80.06	0.123	222.90
L_9_5	1	0.119	7.77	0.119	22.99	0.119	93.06	0.119	261.25
	2	0.116	8.93	0.116	26.84	0.116	106.04	0.116	299.53
	3	0.130	6.72	0.130	19.58	0.130	81.18	0.130	226.49
	4	0.128	7.14	0.128	21.01	0.128	85.91	0.128	240.35
	5	0.127	7.46	0.127	22.00	0.127	89.54	0.127	250.80
AVE	--	0.124	7.60	0.124	22.48	0.124	91.15	0.124	255.68
L_9_9	1	0.126	7.77	0.126	22.99	0.126	93.06	0.126	261.25
	2	0.125	8.09	0.125	24.42	0.125	97.79	0.125	275.11
	3	0.132	7.98	0.132	23.76	0.132	95.37	0.132	268.18
	4	0.121	6.83	0.121	19.91	0.121	82.39	0.121	229.90
	5	0.129	5.15	0.129	14.41	0.129	63.47	0.129	174.13
AVE	--	0.127	7.16	0.127	21.10	0.127	86.42	0.127	241.71
L_9_12	1	0.144	8.30	0.144	24.75	0.144	99.00	0.144	278.63
	2	0.148	8.61	0.148	25.74	0.148	102.52	0.148	289.08
	3	0.145	6.83	0.145	19.91	0.145	82.39	0.145	229.90
	4	0.141	7.77	0.141	22.99	0.141	93.06	0.141	261.25
	5	0.126	8.82	0.126	26.40	0.126	104.83	0.126	296.01
AVE	--	0.141	8.07	0.141	23.96	0.141	96.36	0.141	270.97
L_12_5	1	0.147	9.35	0.147	28.16	0.147	110.66	0.147	313.39
	2	0.153	8.19	0.153	24.42	0.153	97.79	0.153	275.11
	3	0.189	5.36	0.189	17.16	0.189	65.89	0.189	181.06
	4	0.153	7.46	0.153	22.00	0.153	89.54	0.153	250.80
	5	0.152	6.30	0.152	18.26	0.152	76.56	0.152	212.52
AVE	--	0.159	7.33	0.159	22.00	0.159	88.09	0.159	246.58
L_12_9	1	0.161	9.35	0.161	28.16	0.161	110.77	0.161	313.39
	2	0.165	9.56	0.165	28.93	0.165	113.08	0.165	320.43
	3	0.155	9.87	0.155	29.92	0.155	116.71	0.155	330.88
	4	0.156	8.93	0.156	26.84	0.156	106.04	0.156	299.53
	5	0.160	9.77	0.160	29.59	0.160	115.50	0.160	327.36
AVE	--	0.159	9.50	0.159	28.69	0.159	112.42	0.159	318.32
L_12_12	1	0.167	10.29	0.167	31.24	0.167	121.44	0.167	344.74
	2	0.162	10.50	0.162	32.67	0.162	126.28	0.162	358.71
	3	0.169	11.24	0.169	34.32	0.169	132.00	0.169	376.09
	4	0.181	10.92	0.181	33.33	0.181	128.48	0.181	365.64
	5	0.173	9.98	0.173	30.25	0.173	117.81	0.173	334.29
AVE	--	0.170	10.59	0.170	32.36	0.170	125.20	0.170	355.89

Table B 2

Details of the computational results reported in Fig. 8 (midium traffic flow).

Group	Instance	B&P		B&P_No_ISGS		B&P_No_OPVB		B&P_No_HLSA	
		Obj (million)	Time (s)	Obj (million)	Time (s)	Obj (million)	Time (s)	Obj (million)	Time (s)
M_13_13	1	0.340	19.30	0.340	45.54	0.340	153.12	0.340	269.62
	2	0.302	19.91	0.302	47.01	0.302	167.47	0.302	278.09
	3	0.331	19.06	0.331	44.86	0.331	160.23	0.331	266.23
	4	0.322	18.94	0.322	44.64	0.322	159.22	0.322	264.53
	5	0.314	17.12	0.314	40.23	0.314	143.85	0.314	239.11
AVE	--	0.322	18.87	0.322	44.45	0.322	156.78	0.322	263.52
M_13_15	1	0.346	25.98	0.346	61.59	0.346	218.66	0.346	362.39
	2	0.357	25.13	0.357	59.44	0.357	211.42	0.357	350.53
	3	0.348	25.49	0.348	60.46	0.348	214.81	0.348	356.06
	4	0.328	21.25	0.328	50.17	0.328	178.88	0.328	296.96
	5	0.343	21.12	0.343	49.95	0.343	177.75	0.343	295.04
AVE	--	0.344	23.79	0.344	56.32	0.344	200.30	0.344	332.20
M_13_17	1	0.340	25.74	0.340	61.02	0.340	216.85	0.340	359.45
	2	0.337	24.40	0.337	57.86	0.337	205.55	0.337	340.81
	3	0.334	24.52	0.334	58.42	0.334	207.81	0.334	344.54
	4	0.337	21.73	0.337	51.42	0.337	182.95	0.337	303.52
	5	0.346	29.74	0.346	70.85	0.346	251.09	0.346	415.95
AVE	--	0.339	25.23	0.339	59.91	0.339	212.85	0.339	352.85
M_15_13	1	0.325	31.08	0.325	73.90	0.325	261.93	0.325	433.81
	2	0.317	35.69	0.317	85.20	0.317	301.60	0.317	499.23
	3	0.357	27.56	0.357	65.43	0.357	232.22	0.357	384.77
	4	0.351	28.53	0.351	67.80	0.351	240.24	0.351	398.10
	5	0.348	29.74	0.348	70.85	0.348	251.09	0.348	415.95
AVE	--	0.340	30.52	0.340	72.64	0.340	257.41	0.340	426.37
M_15_15	1	0.346	31.08	0.346	73.90	0.346	261.93	0.346	433.81
	2	0.343	32.05	0.343	76.28	0.343	270.30	0.343	447.59
	3	0.363	31.69	0.363	75.94	0.363	269.05	0.363	445.67
	4	0.331	27.19	0.331	64.64	0.331	229.39	0.331	380.25
	5	0.354	20.40	0.354	48.14	0.354	171.65	0.354	285.10
AVE	--	0.347	28.48	0.347	67.78	0.347	240.46	0.347	398.48
M_15_17	1	0.395	33.14	0.395	79.10	0.395	280.01	0.395	463.53
	2	0.406	34.48	0.406	82.15	0.406	290.75	0.406	481.38
	3	0.397	27.19	0.397	64.64	0.397	229.39	0.397	380.25
	4	0.386	32.05	0.386	76.28	0.386	270.30	0.386	447.59
	5	0.346	35.33	0.346	84.19	0.346	297.98	0.346	493.25
AVE	--	0.386	32.44	0.386	77.27	0.386	273.69	0.386	453.20
M_17_13	1	0.403	37.39	0.403	89.38	0.403	316.06	0.403	523.08
	2	0.421	32.78	0.421	77.97	0.421	276.40	0.421	457.54
	3	0.518	23.55	0.518	55.82	0.518	198.32	0.518	328.94
	4	0.421	29.74	0.421	70.85	0.421	251.09	0.421	415.95
	5	0.418	29.74	0.418	70.74	0.418	250.75	0.418	415.39
AVE	--	0.436	30.64	0.436	72.95	0.436	258.52	0.436	428.18
M_17_15	1	0.441	37.39	0.441	89.38	0.441	316.06	0.441	523.08
	2	0.452	38.36	0.452	91.42	0.452	323.29	0.452	534.94
	3	0.426	38.24	0.426	91.30	0.426	322.73	0.426	534.04
	4	0.429	35.69	0.429	85.20	0.429	301.60	0.429	499.23
	5	0.438	39.21	0.438	93.45	0.438	330.53	0.438	546.81
AVE	--	0.437	37.78	0.437	90.15	0.437	318.84	0.437	527.62
M_17_17	1	0.458	41.28	0.458	98.65	0.458	348.49	0.458	576.53
	2	0.444	41.52	0.444	98.88	0.444	349.51	0.444	578.11
	3	0.464	40.30	0.464	96.28	0.464	340.24	0.464	562.85
	4	0.495	43.83	0.495	104.75	0.495	370.19	0.495	612.23
	5	0.475	40.91	0.475	97.75	0.475	345.33	0.475	571.33
AVE	--	0.467	41.57	0.467	99.26	0.467	350.75	0.467	580.21

Table B 3

Details of the computational results reported in Fig. 8 (heavy traffic flow).

Group	In-stance	B&P			B&P_No_ISGS			B&P_No_OPVB			B&P_No_HLSA		
		Obj lion)	(mil-	Time (s)	Obj lion)	(mil-	Time (s)	Obj lion)	(mil-	Time (s)	Obj lion)	(mil-	Time (s)
H_18_18	1	0.735		78.00	0.735		217.14	0.735		506.58	0.735		933.27
	2	0.670		80.34	0.670		223.65	0.670		521.77	0.670		961.23
	3	0.720		77.09	0.720		214.61	0.720		500.56	0.720		922.07
	4	0.705		76.57	0.705		213.29	0.705		497.42	0.705		916.52
	5	0.626		69.68	0.626		193.76	0.626		451.88	0.626		832.53
AVE	--	0.691		76.34	0.691		212.49	0.691		495.64	0.691		913.12
H_18_20	1	0.745		103.61	0.745		288.36	0.745		672.75	0.745		1239.46
	2	0.765		100.36	0.765		279.32	0.765		651.42	0.765		1200.18
	3	0.750		101.92	0.750		283.42	0.750		661.42	0.750		1218.74
	4	0.715		85.54	0.715		238.11	0.715		555.51	0.715		1023.41
	5	0.668		85.02	0.668		236.66	0.668		552.13	0.668		1017.26
AVE	--	0.729		95.29	0.729		265.17	0.729		618.65	0.729		1139.81
H_18_24	1	0.735		102.83	0.735		286.19	0.735		667.57	0.735		1229.82
	2	0.730		97.76	0.730		271.85	0.730		634.07	0.730		1168.37
	3	0.725		98.67	0.725		274.74	0.725		640.82	0.725		1180.54
	4	0.730		87.36	0.730		243.17	0.730		567.31	0.730		1045.22
	5	0.745		118.43	0.745		329.57	0.745		768.67	0.745		1416.24
AVE	--	0.733		101.01	0.733		281.10	0.733		655.69	0.733		1208.04
H_20_18	1	0.710		123.37	0.710		343.18	0.710		800.60	0.710		1475.16
	2	0.695		141.44	0.695		393.43	0.695		917.85	0.695		1691.22
	3	0.765		109.85	0.765		305.71	0.765		713.12	0.765		1313.81
	4	0.755		113.49	0.755		315.83	0.755		736.74	0.755		1357.31
	5	0.750		118.43	0.750		329.57	0.750		768.67	0.750		1416.24
AVE	--	0.735		121.32	0.735		337.54	0.735		787.40	0.735		1450.75
H_20_20	1	0.745		123.37	0.745		343.18	0.745		800.60	0.745		1475.16
	2	0.740		127.14	0.740		353.79	0.740		825.43	0.740		1520.83
	3	0.775		126.62	0.775		352.34	0.775		821.93	0.775		1514.44
	4	0.720		108.55	0.720		302.09	0.720		704.68	0.720		1298.39
	5	0.760		82.29	0.760		229.07	0.760		534.06	0.760		984.12
AVE	--	0.748		113.59	0.748		316.10	0.748		737.34	0.748		1358.59
H_20_24	1	0.831		131.56	0.831		366.08	0.831		853.98	0.831		1573.37
	2	0.851		136.50	0.851		379.82	0.851		885.92	0.851		1632.29
	3	0.836		108.55	0.836		302.09	0.836		704.68	0.836		1298.39
	4	0.816		127.14	0.816		353.79	0.816		825.43	0.816		1520.83
	5	0.745		139.75	0.745		388.85	0.745		907.24	0.745		1671.58
AVE	--	0.816		128.70	0.816		358.13	0.816		835.45	0.816		1539.29
H_24_18	1	0.846		148.07	0.846		411.75	0.846		960.51	0.846		1769.78
	2	0.876		130.00	0.876		361.50	0.876		843.26	0.876		1553.61
	3	1.047		94.38	1.047		262.69	1.047		612.86	1.047		1129.21
	4	0.876		118.30	0.876		329.57	0.876		768.67	0.876		1416.24
	5	0.871		118.30	0.871		329.09	0.871		767.71	0.871		1414.55
AVE	--	0.903		121.81	0.903		338.92	0.903		790.60	0.903		1456.68
H_24_18	1	0.911		148.07	0.911		411.75	0.911		960.51	0.911		1769.78
	2	0.931		151.32	0.931		420.91	0.931		981.83	0.931		1809.07
	3	0.886		151.06	0.886		420.18	0.886		980.27	0.886		1806.30
	4	0.891		141.44	0.891		393.43	0.891		917.85	0.891		4338.00
	5	0.906		154.57	0.906		430.06	0.906		1003.16	0.906		1848.35
AVE	--	0.905		149.29	0.905		415.27	0.905		968.72	0.905		2314.30
H_24_24	1	0.941		162.76	0.941		452.84	0.941		1056.42	0.941		1946.68
	2	0.916		163.28	0.916		454.04	0.916		1059.20	0.916		1951.74
	3	0.951		158.99	0.951		442.36	0.951		1031.96	0.951		4338.00
	4	1.007		172.64	1.007		480.31	1.007		1120.41	1.007		2064.53
	5	0.972		161.33	0.972		448.86	0.972		1047.15	0.972		1929.33
AVE	--	0.957		163.80	0.957		455.68	0.957		1063.03	0.957		2446.05